Aus dem Medizinischen Zentrum für Zahn-, Mund- und Kieferheilkunde
des Fachbereiches Medizin der Philipps-Universität Marburg

Geschäftsführende Direktorin: Prof. Dr. Heike Korbmacher-Steiner

Stiftungsprofessur für Experimentelle Orofaziale Medizin
Leiterin: Prof. Dr. Christine Knabe-Ducheyne

Titel der Dissertation

Effect of a highly bioactive calcium alkali orthophosphate-based bone grafting material as compared to a tricalcium phosphate bone substitute on osteogenesis after sinus floor augmentation in patients

Inaugural-Dissertation

zur Erlangung des Doktorgrades der Zahnmedizin

dem Fachbereich Medizin der Philipps-Universität Marburg

Vorgelegt von

Hana Ayad Ensir
aus Libyen
Marburg, 2020

Angenommen vom Fachbereich Medizin der Philipps-Universität Marburg am 28.10.2020

Gedruckt mit Genehmigung des Fachbereichs

Dekan i.V. der Prodekan: Prof. Dr. R. Müller

Referent: Frau Prof. Dr. C. Knabe-Ducheyne

1. Korreferent: Herr Prof. Dr. S. Ruchholtz

DEDICATED TO
MY BELOVED FAMILY

LIST OF CONTENT

List of Abbreviation:

ARA	**Alveolar Ridge Augmentation**
ALP	**Alkaline Phosphatase**
BG45S5	**Bioglass 45S5**
BCP	**Biphasic calcium phosphate**
BMA	**n-Butyl-methacrylate**
BMI	**Body mass index**
BMPs	**Bone Morphogenic Proteins**
BPO	**Benzoyl peroxide**
BR	**Bone Regeneration**
BSA	**Bovine serum albumin**
BSE	**Spongiform encephalopathy**
BSM	**Bone Substitute Material**
BSP	**Bone sialoprotein**
CaP	**Calcium Phosphate**
CAOP	**Calcium Alkali Orthophosphate**
CBCT	**Cone beam computed tomography**
Col I	**Collagen I**
CMF	**Cranio-maxillofacial**
DFDA	**Demineralized freeze-dried Allograft**
DMT	***N, N*-Dimethyl-*p*-Toluidine**
ECM	**Extracellular matrix**
FDA	**Freeze-dried allografts**
GBR	**Guided bone regeneration**
GFs	**Growth factors**
HA	**Hydroxyapatite**
MMA	**Methyl methacrylate**
OCMF	**Oral and craniomaxillofacial**
OC	**Osteocalcin**
PEG	**Polyethylene glycol**

ROI	**Region of interest**
SFA	**Sinus Floor Augmentation**
SD	**Standard deviation**
SCT	**Synchrotron micro-tomography**
Si	**Silica**
TRAP	**Tartrate Resistant Alkaline Phosphatase**
TGFs	**Transforming growth factors**
TCP	**Tricalcium phosphate**
vWF	**von Willebrand Factor**

Table of Figures:

List of Tables:

1. Introduction

The regeneration of bone tissue represents an important issue in regenerative medicine and tissue engineering. Approximately 1 million patients with bone defects require bone grafting annually, involving the use of appropriate bone substitute materials (BSMs). There furthermore is an increasing demand due to the aging population in both Europe and the United States (Guarino, Causa and Ambrosio, 2007). In addition, the resorptive processes following tooth loss frequently cause alveolar ridge defects (Tonelli *et al.*, 2011). In modern dentistry, the application of dental implants has become a common treatment modality to replace missing teeth and to restore masticatory function. However, sufficient bone volume for anchoring dental implants is often not available, particularly in the posterior maxilla, due to alveolar bone atrophy, poor bone quality or maxillary sinus pneumatization (Starch-Jensen and Jensen, 2017). In such situations, these bone defects need to be restored or augmented (Zerbo *et al.*, 2001). As a result, there has been a considerable increase in alveolar ridge augmentation (ARA) procedures prior to implant insertion over the last 20 years, leading to an increasing demand for adequate BSMs in implant dentistry (Knabe, Ducheyne and Stiller, 2011).

Since the late 70s, a large variety of synthetic BSMs have been developed and proposed as treatments for augmenting the alveolar ridge and inducing bone regeneration (BR) to avoid autograft harvesting (Knabe *et al.*, 2017a). For this purpose, using tricalcium phosphate (TCP) and bioactive glass 45S5 (BG45S5) particles for sinus floor augmentation (SFA) has recently received great interest in oral implantology (Knabe *et al.*, 2008a). However, given that these materials resorb within 1-2 years, intensive studies have been conducted to produce bioactive, highly resorbable BSMs, calcium alkali orthophosphates (CAOP), which show good bone-bonding properties by enhancing osteogenesis in combination with a rapid degradation rate. These materials exhibit a stable and glassy crystalline $Ca_2KNa(PO_4)_2$ phase and display a higher solubility and degradability than TCP (Knabe *et al.*, 2010). More recently, with a silica containing CAOP (Si-CAOP), more enhanced bone formation and particle degradation have been

demonstrated in humans 6 months after SFA when compared with results for polygonal TCP granules (Knabe, *et al.*, 2017b). This Si-CAOP material has been shown to be promising for successful SFA and regenerating maxillary bone defects, potentially reducing the risk of implant failure and facilitating shorter healing times due to its enhanced osteogenic capability. However, there are still clinical considerations for the newly produced BSM in terms of adjusting its chemical and mechanical characteristics to achieve adequate bone ingrowth and neovascularization in the posterior maxilla after *in vivo* implantation. Designing Si-CAOP particles at the molecular scale, within biocompatible, bioactive, and osteoconductive requirements, are the major considerations.

1.1 Dental implants in the posterior maxilla

In recent times, using dental implants as restorations for missing teeth or as rehabilitation for oral and craniomaxillofacial (OCMF) defects has become a standard treatment modality in prosthodontic therapy. However, implant therapy can be challenging for patients with insufficient bone quality and quantity or with osteoporosis (Xie *et al.*, 2012), particularly in the posterior maxilla compromised by sinus pneumatization (Wheeler, 1997). In addition, patients with severe maxillary bone defects commonly have problems with wearing removable dentures, leading to impaired functions and esthetics. In these cases, bone repair is frequently essential (Kaptein *et al.*, 1998). A number of clinical studies conducted on implant survival found that the failure rates of short implants (7-10 mm) were ≥ 35% in the posterior maxilla (Jaffin and Berman, 1991). Thus, the presence of enough bone height and width has been reported as an essential prerequisite to inserting implant-supported prostheses in the edentulous posterior maxilla (Esposito *et al.*, 2010; Xie *et al.*, 2012).

Furthermore, enhancing the bone regeneration process, shortening treatment duration, earlier loading of implants, minimizing patient inconvenience and regular maintenance are considered key factors to ensure the long-term success of implants (Gapski *et al.*, 2003; Xie *et al.*, 2012). The success of implant treatment depends on maintaining an

immediate structural and functional contact between bone tissues and implant surfaces, i.e. osseointegration. Yet, dental implants in the posterior maxilla can fail in the presence of insufficient bone height (Esposito *et al.*, 2009). Today, various techniques are being employed to reconstruct jawbone deficiencies, such as guided bone regeneration, bone grafting, distraction osteogenesis, use of growth factors as well as stem cells (Buser *et al.*, 1999; Titsinides, Agrogiannis and Karatzas, 2019).

Concerted attempts have been made to enhance and augment bone formation around implants by applying various BSMs or/and surface modification technologies (Knabe *et al.*, 2004a; Liu, Chu and Ding, 2004; Xie *et al.*, 2012). Dental implants with adequate surface chemistry and topography have been documented to favour cell adhesion, cell differentiation, and bone tissue formation, and applying appropriate BSM should stimulate the osseointegration process of dental implants (Xie *et al.*, 2012). Correcting bone defects and inserting implants require the use of surgical techniques, which take into consideration the biological healing principles of bone regeneration. However, the volume of the regenerated bone tissue can vary depending on the jawbone anatomy and the patient's metabolic condition (Tonelli *et al.*, 2011).

1.2 Guided bone regeneration

Using osseointegrated implants for the treatment of partially edentulous posterior maxilla has been carefully investigated and well-reported. Guided bone regeneration (GBR) and SFA techniques have been demonstrated to be efficient pre-implantology procedures in the highly resorbed maxilla (Simion *et al.*, 2004). Due to the success of using GBR in implant therapy, implants can now be placed in previously deficient alveolar ridges, with success rates of > 95% reported (Wang and Boyapati, 2006). In addition, a number of studies have shown that GBR could provide > 5mm of horizontal and vertical bone augmentation with long-term implant survival (Buser *et al.*, 1996, 1999; Tinti, Parma-Benfenati and Polizzi, 1996). Currently, GBR is documented to yield ARA with average height of > 8.5 mm in alveolar bone atrophy with average height of 10.0 mm (Funato, Yamada and Ogawa, 2013). Such evidence points to the effectiveness of GBR in improving atrophic bone dimensions (Yamada and Egusa, 2018).

Therefore, GBR has become a firmly established method for improving bone height in the areas planned for implant placement (Buser *et al.*, 1999; Wang and Boyapati, 2006; Knabe *et al.*, 2008a). To ensure the predictability of ARA horizontally and vertically, healing principles of GBR were suggested: primary wound healing, space maintenance and space creation for osteogenic cell growth, angiogenesis stimulation and stability of wound and implant (Wang and Boyapati, 2006) (Figure 1-1). The primary role of BSMs as scaffolds, in addition to space maintenance, is to attract osteoprogenitor cells and enhance their differentiation into terminally differentiated osteoblasts, which produce mineralized bone matrix. Hence the host response is a crucial factor for the success of GBR (Yamada and Egusa, 2018).

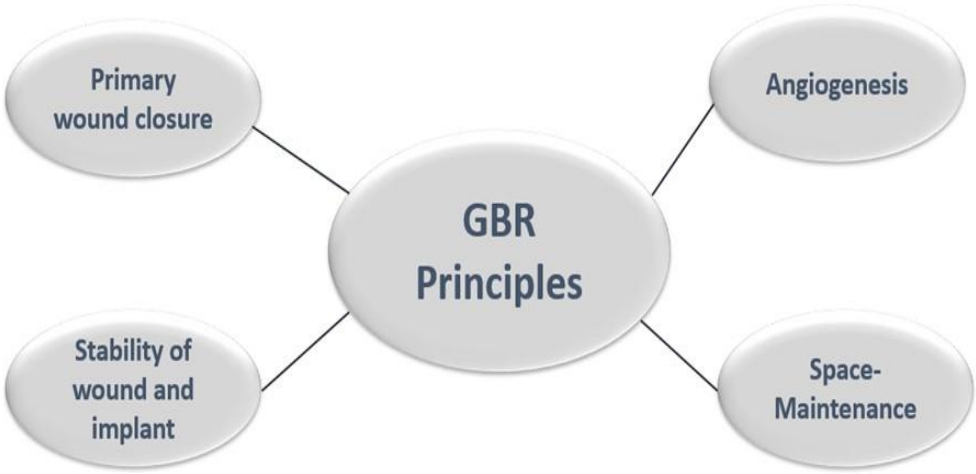

Figure 1-1: Biological principles of GBR protocol

1.3 Sinus floor augmentation

Sinus augmentation, previously called sinus lifting, is an internal augmentation of the maxillary sinus floor by use of various BSMs, aiming to enhance bone growth, and therefore increase the vertical height of bone in the posterior part of the maxilla before or in combination with insertion of the implant (Van Den Bergh *et al.*, 2000; Starch-Jensen and Jensen, 2017). This pre-prosthodontic surgical technique, which was introduced by Tatum (Tatum, 1986), explained by Boyne and James (Boyne and James, 1980) and later modified by Wood and Moore, has increasingly been shown to facilitate

the successful use of implants in the posterior maxilla (Van Den Bergh *et al.*, 2000). The procedure requires preparation of an access window in the lateral wall of the sinus through a buccal incision and elevation of the mucosal lining, i.e. the Schneiderian membrane, thereby creating a space in which the BSM is placed and left to heal for 6 months before installing the implant (Esposito *et al.*, 2010). While the principle of this procedure seems simple, there are a number of anatomical aspects of the maxillary sinus that should be considered in relation to this surgery (Van Den Bergh *et al.*, 2000).

Many reports based on reliable clinical statistics have expressed general agreement with the surgical approach for the sinus floor, but there has been considerable disagreement relating to the use of BSMs (Wheeler, 1997). Some local and systemic conditions could compromise the bone healing process and implant osseointegration. As a result, the sinus floor should be carefully evaluated before planning SFA. Acute and chronic sinusitis, tumors, previously destructive sinus operations, and smoking are regarded as contraindications to sinus augmentation (Van Den Bergh *et al.*, 2000; Katranji, Fotek and Wang, 2008). Hence medical history, clinical examination, and pre-operative radiographs are crucial for treatment planning to avoid possible complications (Van Den Bergh *et al.*, 2000). To this end, the presurgical assessing of bone volume, understanding of the variation in the sinus anatomy and choosing the right BSM are of great relevance for the success of SFA procedures and primary stability of implant therapy.

These procedures require sinus grafting with a material that facilitates regeneration of bone that is structurally and functionally similar to the original bone. These regenerative techniques are a basis for correcting horizontal and vertical bone loss and for creating suitable bone quantity and quality for oral rehabilitation (Zizzari *et al.*, 2016).

The quantity and quality of alveolar bone at the implantation sites have been considered major factors affecting the clinical success of implant osseointegration. According to the literature, quantity includes the height, width, and morphological features of bone, whereas quality includes bone density (Drage *et al.*, 2007). Implant insertion can be associated with SFA as a one-stage technique, in which an implant can be placed

immediately if there is adequate bone height (> 4.0 mm), or as a two-stage technique, in which the implant needs to be inserted in a second stage, 4 or 6 months after sinus grafting, if there is a lack of sufficient bone quality or quantity (< 4.0 mm) (Van Den Bergh *et al.*, 2000). However, external factors such as initial implant stability, surgical technique, and infection control could partially affect the outcomes of the implants (Temmerman *et al.*, 2015). As a consequence, in addition to the assessment of alveolar bone in terms of evaluating the sinus anatomy and present bone features, the entire treatment process needs to be planned carefully in order to achieve long-term esthetic and functional rehabilitation with implants (Clark and Levin, 2016; Göçmen and Özkan, 2017).

1.4 Bone substitute materials

The bony augmentation of the sinus floor by insertion of BSM is a superior method to create an adequate bone volume for implant placement (Suba *et al.*, 2006). The BSMs are either of natural or synthetic origin and used for grafting in the bone defect regions and can vary concerning their osteogenic properties (Misch and Dietsh, 1993; Titsinides, Agrogiannis and Karatzas, 2019). BSMs can be osteogenic, osteoconductive and osteoinductive (Tonelli *et al.*, 2011; Titsinides, Agrogiannis and Karatzas, 2019) (Table 1-1). Implant bone grafting materials which act as scaffolds for bone formation along their surfaces are considered as osteoconductive (Misch and Dietsh, 1993).

Table 1-1: Biological principles of the bone healing process

Principles	Description
• **Osteogenesis**	• The capability for new bone formation by osteoblasts within the BSM.
• **Osteoconduction**	• The capability to serve as a template to form new bone.
• **Osteoinduction**	• The capability to induce differentiation of mesenchymal stem cells into bone forming-osteoblasts.

A variety of BSMs were used for maxillary SFA (Starch-Jensen and Jensen, 2017) and classified according to their source of origin into the following types (Table 1-2): autograft (obtained from the same person), allograft (obtained from another person), xenograft (obtained from different species), and alloplastic graft (synthetic material) (Misch and Dietsh, 1993; Zizzari *et al.*, 2016; Turco *et al.*, 2018; Titsinides, Agrogiannis and Karatzas, 2019). While there is a wide range of available biomaterials, controversy over the ideal BSM has persisted for many years (Starch-Jensen and Jensen, 2017). There is, however, agreement that BSMs for bone reconstruction should have specific properties, including bone-healing properties, stimulation of vascularization, absence of adverse host reactions, high availability, low morbidity, stability and solubility, easy handling and cost-effectiveness. Intensive work is needed to meet these requirements, given that an ''excellent'' BSM has not yet been designed (Titsinides, Agrogiannis and Karatzas, 2019).

Table 1-2: Advantages and disadvantages of the bone substitute materials used in oral and maxillofacial surgery (Turco *et al.*, 2018)

B.S.M	Advantages	Disadvantages
• Autografts	• Osteoconductive • Osteoinductive • No disease transmission & immunological response • Low cost	• High morbidity • Low availability • Limited dimensional stability
• Allografts	• Osteoconductive • High availability • Low morbidity	• Minor wound complications • Limited volumetric stability • Disease transmission & • Immunogenicity • High cost
• Xenografts	• Osteoconductive • High availability • High dimensional stability • Low morbidity	• No osteoinductivity • Disease transmission & immune response • High cost
• Synthetic bone materials	• Osteoconductive • Some are bioactive • High availability • Changeable dimensional stability • Low morbidity • No disease transmission	• In most cases no osteoinductivity • Risk of immune response • High cost

1.4.1 Requirements for BSMs

In material science, fulfilling the ideal requirements for BSMs appears to be a challenge. However, great efforts have been made to develop highly biodegradable biomaterials, which facilitate restoring the mechanical and functional properties of bone tissue, thereby providing support for implant-supported prostheses and improving the oral health-related quality of life (Guarino, Causa and Ambrosio, 2007). The BSM should be

biocompatible, biodegradable, and bioactive, with suitable chemical and mechanical properties and without any antigenic reactions (Table 1-3) (Zizzari *et al.*, 2016).

Table 1-3: The main requirements for BSMs

Requirements	Description
• Biocompatibility	• The ability of the BSM to stimulate osteogenesis without adverse host reactions.
• Biodegradability	• The capability to produce newly functional replacement bone tissue via chemical dissolution and for osteoblasts to remodel bone.
• Bioactivity	• The capability to attract osteoprogenitor cells to its surface and to enhance osteoblasts differentiation and bone matrix and bone tissue formation.

To regenerate bone, the BSMs should perform the following functions: acting as a temporary scaffold for osteogenesis, allowing for nutrient and growth factors transportation, as well as providing an approximation of the biodegradation rate with the rate of bone formation (Yamada and Egusa, 2018). The application of BSMs has been the most common approach to enhance bone formation at the implant sites. However, there are still several aspects that need to be better understood concerning their clinical uses for bone augmentation (Xie *et al.*, 2012). While structural features were reported to cause suitable biological integration, physical and chemical features are regarded as principle aspects for cell adhesion and proliferation (Turco *et al.*, 2018). Therefore, it is essential to understand the mechanical, chemical, and physical properties of the BSMs in order to choose appropriate biomaterials for ARA (Figure 1-2) (Zizzari *et al.*, 2016).

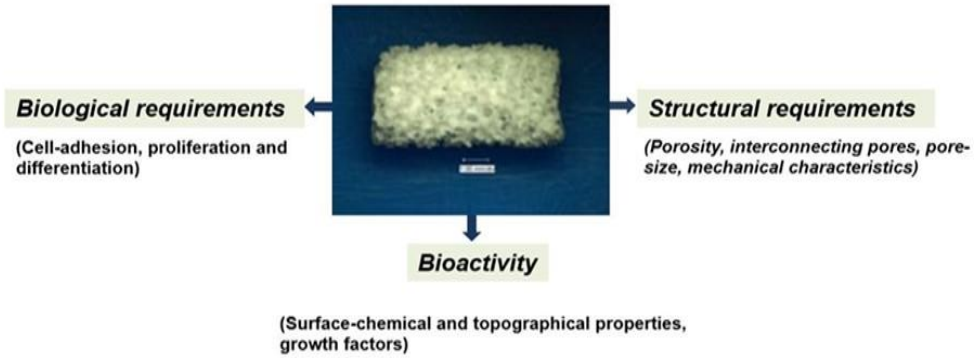

Figure 1-2: Schematic diagram of the major requirements for synthetic BSMs

1.4.2 Types of BSMs

1.4.2.1 Autogenic bone grafts

Autografts, either particulate or block, are still regarded as the most efficient BSMs for bone repair due to their higher biocompatibility, reliability, and osteogenic potential (Wheeler, 1997; Moore, Graves and Bain, 2001; Zizzari *et al.*, 2016; Turco *et al.*, 2018). Regardless of these benefits, there are a number of drawbacks, including donor site morbidity, need for an additional surgical site, bone volume that can be harvested is limited, and risk of chronic pain (Moore, Graves and Bain, 2001; Knabe *et al.*, 2008a; Turco *et al.*, 2018).

The development of postoperative sinusitis has been detected, which may affect the outcomes of sinus grafting or implant treatment (Timmenga *et al.*, 1997). Hence various BSMs have been applied widely to simplify the operative procedures and avoid bone harvesting (Starch-Jensen and Jensen, 2017).

The donor regions can be located intraorally: chin, tuberosity, and ramus, or extra orally: iliac crest, calvarias, and tibia (Misch and Dietsh, 1993; Zizzari *et al.*, 2016). Nearly 8% of iliac crest grafts have reportedly resulted in infection, bleeding, arterial and nerve

injuries, hematoma, short- or long-term pain, and function loss (Wheeler, 1997). Moreover, 151 iliac bone grafts were harvested with clinical follow-up over 12 months and it was found that at 29% of these sites there was persistent chronic pain lasting for 3 months (Fernyhough *et al.*, 1992). To overcome these limitations, the search for an adequate bone replacement material which would avoid the need for an additional operative site is ongoing (Wheeler, 1997).

1.4.2.2 Allografts

Allogenic grafts as alternatives are based on the same principles as autografts, with exclusion of the osteogenic principle. They are collected from cadavers and used for large bone defects and where there is insufficient autograft volume (Moore, Graves and Bain, 2001). Decreased operative-time and anaesthesia with less blood loss could be advantageous features for such grafts (Misch and Dietsh, 1993). While the major risks of this form of graft were reported mostly as bacterial infection and viral transmission, the fracture rate in allografts was at about 19% (Moore, Graves and Bain, 2001). The use of freeze-dried allografts (FDA) and demineralized freeze-dried allografts (DFDA) have been proposed and possibly form bone by osteoconductive mode (Misch and Dietsh, 1993; Titsinides, Agrogiannis and Karatzas, 2019). Thus, bone formation is likely to be slower than in the case of autografts (Misch and Dietsh, 1993).

1.4.2.3 Xenografts

Xenografts are also considered as substitutes for autografts, for instance, bovine, equine and porcine biomaterials (Turco *et al.*, 2018). Despite the popularity of bovine grafting biomaterials in maxillofacial surgery, there is a strong link between disease transmission and xenografts. On the one hand, it was proposed that the risk of bovine spongiform encephalopathy was correlated to the processing of raw bovine bone but not to bovine bone substitutes (Sogal and Tofe, 1999). On the other hand, a systemic review concluded that a risk of prion transmission to patients could be attributed to bovine bone grafts, despite no currently available research having quantified the risk (Kim, Nowzari and Rich, 2013).

1.4.2.4 Synthetic bone materials

These biomaterials were recognized as bone substitutions in the early 1980s (Wheeler, 1997), for their osteoconductive and bioactive properties and exclusion of the need for additional surgical sites and the risk of disease transmission. They have been increasingly used for medical applications and are available in different sizes and shapes (Turco *et al.*, 2018; Titsinides, Agrogiannis and Karatzas, 2019). In addition, osteoinductive properties can be endowed by introducing growth factors (GFs), namely transforming growth factors (TGFs) or bone morphogenic proteins (BMPs-2, 7), to their inner structures, outer surface or interfacial sites (Xie *et al.*, 2012). Over 20 years, several preclinical studies have established the use of BMP 2 and BMP 7 for bone regeneration in OCMF applications (Knabe *et al.*, 2017a).

The construction of these BSMs depends on their capability to simulate the characteristics of native bone and serve as three-dimensional scaffold for cell ingrowth, and subsequent osteogenesis (Zizzari *et al.*, 2016). In this context, several strategies were employed to stimulate BR within the biomimetic BSM, including producing a BSM with specific surface topography, forming mineralized layers, or using bioreactors. Such approaches allow mimicking of the natural environment for osteoblasts to grow normally (Zizzari *et al.*, 2016; Titsinides, Agrogiannis and Karatzas, 2019). Besides the mechanical properties, geometry, chemical composition and ultrastructure of the synthetic BSMs are determining parameters for successful bone healing, while their ability to resorb *in vivo* is valuable for achieving complete replacement of these biomaterials with newly formed bone (Zizzari *et al.*, 2016; Titsinides, Agrogiannis and Karatzas, 2019). According to some studies, the geometric design of these biomaterials, particularly hydroxyapatite-based (HA) and biphasic calcium phosphate (BCP), triggers cell differentiation and intrinsic stimulation of osteogenesis by the bioactive and biomimetic properties (Zizzari *et al.*, 2016).

Intensive research has been done to describe and characterize the BSMs, which tested their biocompatibility and efficiency on cell colonization in several *in vitro* experiments (Turco *et al.*, 2018). The mechanical stability and porosity should be in the right balance

to design BSM architecture. To enhance biodegradation, osteogenesis, and vascularization, the porosity should be open, of 200 to 400 µm in diameter, with higher rates of interconnectivity (Zizzari *et al.*, 2016; Turco *et al.*, 2018; Titsinides, Agrogiannis and Karatzas, 2019). Hence, to ensure such functions, these substitutes should have different levels of porosity for various length structures: millimeter-pores for blood and nerve vessel growth, micro-pores for the capillary formation and cell migration, and nano-pores for nutrition and waste transportation (Zizzari *et al.*, 2016).

The majority of the synthetic BSMs are bioceramics, including calcium phosphate-based (CaP) biomaterials (Misch and Dietsh, 1993; Gaviria *et al.*, 2017) and bioactive glasses (BG) (Bunte and Strunz, 1977; Knabe *et al.*, 2017a). These bioceramics are valid alternatives to autografts and allografts for use in sinus grafting. CaP biomaterials have been intensively used for dental and CMF repair for several decades (Xie *et al.*, 2012), representing attractive candidates due to their superior biocompatibility; bioactivity; osteoconductivity, bioresorbability, compositional similarity to the native bone, as well as their ability to trigger cell-signaling of osteogenesis (Xie *et al.*, 2012; Gaviria *et al.*, 2017; Thrivikraman *et al.*, 2017; Turco *et al.*, 2018).

The most widely examined CaP bioceramics are HA, β-TCP and BG45S5 (Yaszemski *et al.*, 1996; Knabe *et al.*, 2017a); present most commonly in particulate form, they are also available in blocks or porous blocks (Thrivikraman *et al.*, 2017). Although the mechanism of CAOP-stimulated BR is not yet fully explained, there has been promising pre-clinical data showing the effect of CaP ceramics on craniofacial bone (Thrivikraman *et al.*, 2017). For instance, β-TCP and CAOP substitutes have been clinically reported as having high success rates and serving as superior alternative BSMs to autografts (Knabe *et al.*, 2008b, 2014, 2017b, 2018). Yet, considerable efforts have been focused on increasing the osteogenic capacity of these BSMs for a shorter duration and, eventually, to facilitate placement of the dental implant at an earlier time point (Knabe *et al.*, 2018).

a) Hydroxyapatites

HA biomaterials ($Ca_{10}(Po_4)_6(OH)_2$; Ca/P ratio=1.67), either synthetic or natural, are the most stable orthophosphates (Dorozhkin and Epple, 2002) and possess superior biocompatible and osteoconductive properties (Titsinides, Agrogiannis and Karatzas, 2019). They can be categorized according to the porosity percentages as dense, microporous, or macro-porous, and as amorphous or crystalline in form. The crystalline form has higher fracture resistance than the amorphous form. Small sized HA crystals seem preferable because they enhance the biomaterial-bone contact (Zizzari *et al.*, 2016). Some authors argued that new bone, when formed into porous HA, cannot undergo remodeling. This would be possible if these BSMs were to degrade and allow loading of bone. Meanwhile, others have reported that in composition, it simulates natural bone HA more closely than does β-TCP (Yaszemski *et al.*, 1996).

In vitro, microscopic examinations showed the colonization of polygonal cells within a week of culture, and the initial extracellular matrix (ECM), suggesting HA is itself highly bioactive (Mastrangelo *et al.*, 2008), whereas when a non-resorbable porous type of HA was tested *in vivo* for SFA and compared to sites with autografts, no significant variations were found in bone-biomaterial contact. Therefore, it was considered advisable to use HA in combination with autologous bone for SFA (Zizzari *et al.*, 2016). Furthermore, in a human study, nano-crystalline porous HA was completely resorbed and physiologically remodeled during bone healing. In spite of that, slow resorbability, brittleness and low fracture strength are regarded as drawbacks for these HA crystals (Zizzari *et al.*, 2016). Highly crystallized HA was found to be present in unchanged form in a defect years after the implantation. Therefore, β-TCP and biphasic calcium phosphate (BCP) were considered preferable (Dorozhkin and Epple, 2002).

b) Tricalcium Phosphates

TCP ceramics ($Ca_3(PO_4)_2$; Ca/P=1.5), such as Cerasorb®, were developed in the early 1970s, are found either as stable phase, β-TCP phase, or reactive phase, α-TCP (Dorozhkin and Epple, 2002; Peters and Reif, 2004). They were commonly used as alloplastic BSMs because of their biocompatible and osteoconductive properties

(Titsinides, Agrogiannis and Karatzas, 2019). The examined β-form of TCP granules are smaller in size and have shown higher degradability, higher microporosity, and lower mechanical stability than the α-form of TCP (Merten *et al.*, 2001). These properties have been shown in both cell cultural experiments and clinical studies. As a three-dimensional (3D)-scaffold, the β-form provides a better environment for osteoblast adhesion, proliferation, and differentiation, as well as serves as a nucleator of Ca/P precipitation and apatite crystal formation for improving BR (Liu *et al.*, 2008).

The β-TCP ceramics have been historically well accepted as BSMs for sinus augmentation (Zerbo *et al.*, 2004). In the past, the TCP types were frequently contaminated, and therefore, the time needed for their degradation was relatively variable (Merten *et al.*, 2001). These time differences may be attributed to the differences in macro- and meso-porosity, interconnectivity, grain size, and crystallinity of the TCP granules (Stiller *et al.*, 2009). In recent times, TCP has been improved to produce a phase purity of > 99 % with homogenous solubility to prevent the premature decomposition into small particles (0.56% µm). These micro-particles have been previously shown to provoke inflammatory tissue reactions (Peters and Reif, 2004; Knabe and Ducheyne, 2008; Knabe *et al.*, 2017a). To minimize this, the predictable size of micro-particles should be around 7-10 µm (Peters and Reif, 2004).

Cerasorb®, as a granulate or block, is made from a phase pure β-TCP (Ca_3 $(PO_4)_2$) synthesized by a solid reaction of calcium carbonate $CaCO_3$ and calcium hydrogen phosphate $CaHPO_4$ (Peters and Reif, 2004). This form has a porous structure with a spherical shape (Zerbo *et al.*, 2001). Biodegradation and the osteogenic potential of different β-TCP modifications (Cerasorb® Granulate, Cerasorb® Block Forms, Cerasorb® PARO and Cerasorb® M) may be influenced by the phase purity, particle size, porosity, microstructure, stability and chemical solubility (Peters and Reif, 2004; Stiller *et al.*, 2009; Knabe *et al.*, 2017c). Hence, using β-TCP particles with increased porosity has been proposed to increase the biodegradation process (Peters and Reif, 2004; Knabe *et al.*, 2008b; Stiller *et al.*, 2009). Such particles exhibit pores designed with different length structures to decrease bulk density, including macroporosity for osteogenesis and

vascularization, mesoporosity for cell and nutrients transportation, and microporosity for fluid circulation and increasing the surface area (Peters and Reif, 2004; Knabe *et al.*, 2017a).

In evaluating the effect of Cerasorb® on osteogenesis, noteworthy studies have shown its suitability as a BSM for SFA. However, the rates of biodegradation and bone formation seem low compared to those sites augmented with autogenous bone (Zerbo *et al.*, 2004). Similarly, human biopsies at 6 months after SFA have been histologically documented as being incompletely degraded, composed of 38% mineralized bone and 8-26% remaining particles (Szabó *et al.*, 2005). Subsequently, two particulate TCPs with different porosity (35% and 65%) were studied using patient biopsies, revealing that large size combined with high porosity of these particles appears beneficial for enhancing biodegradability and osteogenesis (Knabe *et al.*, 2008b), and further guaranteeing bone formation within their pores (Liu *et al.*, 2008). Moreover, using TCP with additives such as zinc or silica has been introduced to increase its osteogenic efficiency and mechanical characteristics (Bohner, 2009).

More recently, Stiller *et al*. have found that the putty-type of TCP, consisting of pure phase β-TCP granules with two ranges of grain size (125-250 µm; 500-700 µm) and embedded in hyaluronic acid carrier, offers better handling in operative procedures for SFA and histomorphometrically higher bone formation compared to the granular type (Stiller *et al.*, 2014; Knabe *et al.*, 2017c). Nevertheless, there were significant differences in the amount of bone formation between the two material types. Therefore, further research is needed to clarify whether this influence may be associated with the addition of hyaluronic acid or with the different particle sizes of the putty type (Knabe *et al.*, 2017c). In 2015, the *in vivo* performance of paste and foam types of TCP were also studied, showing greater resorption and BR with better surgical handling properties for clinical applications compared to the granular type (Lopez-Heredia *et al.*, 2014).

Interestingly, a clinical study conducted by Knabe *et al*. has examined the effect of host factors on BR and osteogenic marker expressions after SFA using β-TCP. The histological analysis displayed higher levels of body mass index (BMI) and estradiol (E2) in male patients and enhanced TCP-mediated BR in the sinus floor. The histomorphometric

assessment furthermore disclosed a trend toward greater BR and osteogenic marker expression in non-smokers compared to smokers. Hence, this study generated comprehensive knowledge regarding how patient host factors, such as hormones and BMI, could affect the osteogenic potency of these ceramics (Knabe *et al.*, 2017d).

Accordingly, the use of β-TCP in several clinical cases has been successfully reported in both implant dentistry and CMF surgery (Szabó *et al.*, 2005). Therefore, it can be considered as a suitable BSM for different clinical applications such as SFA (Stiller *et al.*, 2014). Even so, research is still ongoing to improve the resorbability rate of the CaP substitutes in the sinus floor.

c) Biphasic Calcium Phosphates

BCP, first described by Nery *et al*., consists of a mixture of HA and β-TCP in different ratios to achieve the desired absorption rate and mechanical properties (Nery *et al.*, 1992; Jensen *et al.*, 2007; Titsinides, Agrogiannis and Karatzas, 2019). BCPs are characterized by biodegradability, high biocompatibility and osteoconductivity, with sufficient mechanical strength for bone repair. These properties depend on achieving the right balance between the high-soluble TCP and the low soluble HA (Zizzari *et al.*, 2016). By altering the crystallinity of BCP or the composition of HA/β-TCP ratio, the bioactivity of these bioceramics can be tailored to induce bone formation. Therefore, BCPs are clinically recommended for orthopedic and oral surgery (Legeros *et al.*, 2003; Jensen *et al.*, 2007; Zizzari *et al.*, 2016). In evaluation of BCP's osteogenic efficiency, *in vitro* and *in vivo* studies with different HA-TCP concentrations have demonstrated that osteoblastic attachments onto the CaP surface are significantly affected by the ratio of TCP component (Jensen *et al.*, 2007). For example, histologic analysis on the repair of bone defects in minipig mandibles revealed that the degradation rates of BCP (60% HA: 40% TCP) and pure HA were relatively slow within two years when compared to that of beta-TCP, which exhibited faster and complete resorption within eight months. This evidence proved that the rate of new bone formation is related to the composition of TCP in these CaP ceramics (Jensen *et al.*, 2007). Despite the incomplete biodegradation, BCP exhibited greater bioresorbability in the sinus floor than the bovine-derived HA

materials (Bio-Oss®). However, since this was correlated with less bone bonding behavior, further investigations on the different resorption properties of BCP were considered essential (Cordaro *et al.*, 2008).

d) Bioglass 45S5

BG45S5, first discovered in 1969 (Hench *et al.*, 1971), is composed of silicate-based glasses (SiO_2, Na_2O, CaO, P_2O_5), and has shown superior osteoconductivity and strong bone-bonding behavior (Knabe and Ducheyne, 2008; Hench, 2015; Titsinides, Agrogiannis and Karatzas, 2019), but its mechanical properties are low (Zizzari *et al.*, 2016). This drawback has been addressed by the addition of synthetic polymer to BG, which has led to enhancement of these properties and prolonged the degradation time during BR (Zizzari *et al.*, 2016). Its absorption rate appeared variable and reliant on the comparative amounts of the glass components (Titsinides, Agrogiannis and Karatzas, 2019). In a comprehensive histomorphometric study, biodegradation of BG45S5 of narrow size range has been reported to be at 12-24 months after human SFA (Tadjoedin *et al.*, 2002). However, by using a mixture of BG (80%-90%) and autograft (10%-20%), the formation of new bone could be observed after 6 months (Zizzari *et al.*, 2016). Thus, compared to the clinically used β-TCP, there is a significant demand for a BSM that stimulates osteogenesis in combination with high degradation rate (Knabe *et al.*, 2008a). Therefore, ideally a bone substitute material should stimulate bone formation at its surface, resorb within the newly formed bone and be replaced by fully functional new bone tissue resulting in restoration of the original osseous microarchitecture within a limited time frame.

e) Calcium Alkali Orthophosphates

Over two decades, intensive research has been carried out on CAOP-based ceramics as highly resorbable BSMs (Berger, Gildenhaar and Ploska, 1995; Knabe *et al.*, 2008a). They have been designed to crystallize immediately from the melt, containing glassy and crystalline CAOP. The main crystalline phase is composed of novel synthesized stable $Ca_2KNa(PO_4)_2$ or $Ca_{10}[K/Na]\ (PO_4)_7$ phases (Berger, Gildenhaar and Ploska, 1995; Knabe *et al.*, 2017a). These ceramics are developed to produce a higher chemical solubility and

biodegradability than β-TCP and consequently could be ideal as alloplastic agents for ARA. CAOPs have a high melting temperature (>1700°C) resulting from the addition of MgO and SiO_2 (Berger, Gildenhaar and Ploska, 1995).

The rate of their biodegradability can be enhanced by addition of diphosphates, which results in formation of amorphous or crystalline diphosphates. Diphosphates ($Ca_2P_2O_7$) are reported to have higher solubility compared to orthophosphates (Knabe *et al.*, 2008a), and to be initially deposited *in vivo* during bone matrix mineralization (Roberts *et al.*, 1992). Numerous studies, both *in vitro* and *in vivo,* have examined CAOPs with diphosphates and achieved promising results on their ability to regenerate bone, leading to the development of CAOP with a small component of diphosphates (Berger, Mücke and Harbich, 2003). From these ceramics, 3D scaffolds can be fabricated which are considered beneficial for craniofacial tissue engineering approaches (Knabe *et al.*, 2008a, 2017a).

The addition of Si into the crystalline structure of various CaP ceramics such as HA and β-TCP has been proposed, generating materials with better biological performance compared to their stoichiometric counterparts (Pietak *et al.*, 2007; Bohner, 2009). Moreover, Yao *et al*. found that Si containing BG45S5 had a greater effect on bone formation and release of Si^{4+} and Ca^{2+} ions products (Yao *et al.*, 2005). A Si-3D printed scaffold has been reported not only to stimulate bone cell differentiations *in vitro*, but also to stimulate osteogenesis and angiogenesis (Knabe *et al.*, 2018). Recently, it has been proved that silica-based CAOPs also enhanced angiogenesis in *in vivo*, providing interesting perspectives for their applications in bone defect repairs (Zhai *et al.*, 2012). Notably, Si-doped CAOP with the main phase of $Ca_2KNa(PO_4)_2$ has demonstrated greater osteoblastic proliferation, differentiation and bone regeneration compared to other CAOP compositions (Knabe *et al.*, 2008a, 2017a; Knabe, Adel-Khattab and Ducheyne, 2017). In addition, Si-doped CAOPs implanted in a sheep scapula have induced considerably increased bone formation with particulate degradation in the grafted defects at shorter healing times, followed by β-TCPs and Si-TCPs (Knabe *et al.*, 2014, 2018).

Many human studies in BR have included clinical and radiographic observations. Nevertheless, the most efficient way of evaluating the effectiveness of these materials on bone formation is to use histological tissue sections from samples harvested in the augmented regions (Zerbo *et al.*, 2001). As a result, in the prospective study, we have carried out histological, histomorphometric, immunohistochemical evaluation of biopsies harvested at dental implant placement at six months after grafting with the Si-CAOP material for comparison with the widely used TCP material. Since when using a staged approach for SFA newly regenerated bone tissue needs to be removed for preparing the implant bed at dental implant placement, the removed tissue, which normally would be discarded can be used for histologic evaluation without violating any accepted ethical standards for patient care.

1.5 Aim of the study

The ultimate goal of the current clinical study is to generate data resulting from both clinical and detailed histological, histomorphometric, and immunohistochemical analysis regarding the efficacy of the highly resorbable Si-CAOP material for bone regenerative therapies in implant dentistry in humans.

Objectives

Surgical objectives:

i. To augment maxillary sinus floors of 12 patients with Si-doped CAOP particles.

ii. To insert dental implants and to sample biopsies at the implant sites 6 months after SFA surgery.

Laboratory objectives:

iii. To process all samples for hard tissue histology, immunohistochemical analysis, and histomorphometrical evaluation.

iv. To examine the effect of Si-CAOP particles on bone tissue formation and osteogenic marker expression (osteocalcin, collagen type I, bone sialoprotein, and alkaline phosphatase) and eventually to compare this effect to that of β-TCP in 12 patients obtained 6 months after SFA.

v. To establish a technique for immunohistochemical detection of an angiogenic marker (von Willebrand factor) in resin embedded biopsy sections (proof-of-concept experiment).

2. Materials and Methods

2.1 Bone substitute materials used:

Two synthetic CaP based BSMs were investigated in the current study. The materials were available as particles produced by Curasan AG, Germany.

2.1.1 Osseolive™ particles

It is a silica-containing calcium alkali orthophosphate granules (Si-CAOP, Osseolive™), with the main glassy crystalline phase ($Ca_2KNa(PO_4)_2$) and an amorphous component, i.e. 4% of sodium magnesium silicate. Its open-pore grains are characterized by high resorbability. It has received the CE mark in 2011 and was approved by the FDA in 2013. The material characteristics have been described in vast detail in a recent publication (Knabe *et al.*, 2018).

2.1.2 Cerasorb™M particles

Cerasorb M particles are a pure phase ≥ 99% beta-tricalcium phosphate granules (β-TCP, Cerasorb™ M, $Ca_3(PO_4)_2$). It has multiple and irregular porous structure to enhance the osteoconductivity. The composition and material characterization of both used BSMs based on the manufacturer's information are listed in Tables 2-1 and 2-2 (Knabe *et al.*, 2018).

Table 2-1: Composition of Si-CAOP and β-TCP materials tested (Knabe *et al.*, 2018)

Test material	Composition (wt %)					
	Ca	**K_2O**	**Na_2O**	**PO_4**	**MgO**	**SiO_2**
Si-CAOP (Osseolive) $Ca_2KNa(PO_4)_2$	22.5±2	13.7±2	9.6±2	48.4±3	2.8±2	3.0±1
β-TCP (Cerasorb M) $Ca_3(PO_4)_2$	38.8±1	-	-	61.2±1	-	-

Table 2-2: Characterization of Si-CAOP and β-TCP particles (Knabe *et al*., 2018)

BSM	Description	Grain size	Pore size	Porosity
Si-CAOP	Open cellular Rough surface Round +large boundaries Regular and open microarchitecture	1000 – 2000 µm	250-450 µm	75%
β-TCP	Porous Smooth surface Straight +Small boundaries Irregular and Close Microarchitecture	1000 – 2000 µm	0.1-500 µm	65%

2.2 Patient selection

A total of 24 partially edentulous patients (12 women and 12 men), between the ages of 39 and 71 years (mean 57), were chosen for SFA and dental implant placement in the posterior maxilla using BSMs. The Freiburg Ethics Commission approved the study in 2013 (Study Code: ZD-MA-MS-2013-1, Ref. Nr. 013/1294). The inclusion criteria include healthy patients with a width of the alveolar ridge of > 6 mm. Any case with the following criteria: clinical or radiological sinus pathologies, active periodontitis, serious systemic diseases, drug abuse and recent chemotherapy, were excluded from the current study. The patient data are shown in Table 2-3. None of the selected patients were smokers; only one patient had a history of smoking 0-5 cigarettes daily. All participants received full information about the treatment plan, including SFA procedures, BSMs and dental implant, and provided their informed consent.

SFA surgery was required for all examined participants with the purpose of inserting dental implants in the augmented areas. An experienced surgeon carried out the first and second surgical procedures. The participants were divided into two equal research groups; group A of 12 patients implanted with Si-CAOP Osseolive particles, whereas group B of 12 patients served as a control group and received β-TCP Cerasorb M particles, allowing evaluating and comparing both materials. The study was performed in a period of two years.

Table 2-3: Clinical patient data

Group A	Age Years	Gender	B.S.M
1	51	*M	Si-CAOP Osseolive™
2	51	M	Si-CAOP Osseolive™
3	67	*F	Si-CAOP Osseolive™
4	71	M	Si-CAOP Osseolive™
5	51	F	Si-CAOP Osseolive™
6	70	F	Si-CAOP Osseolive™
7	69	F	Si-CAOP Osseolive™
8	68	M	Si-CAOP Osseolive™
9	66	F	Si-CAOP Osseolive™
10	51	F	Si-CAOP Osseolive™
11	70	M	Si-CAOP Osseolive™
12	59	M	Si-CAOP Osseolive™
Group B			
1	55	M	β-TCP Cerasorb™M
2	65	M	β-TCP Cerasorb™M
3	60	F	β-TCP Cerasorb™M
4	65	M	β-TCP Cerasorb™M
5	60	M	β-TCP Cerasorb™M
6	47	F	β-TCP Cerasorb™M
7	44	M	β-TCP Cerasorb™M
8	44	F	β-TCP Cerasorb™M
9	48	M	β-TCP Cerasorb™M
10	47	F	β-TCP Cerasorb™M
11	39	F	β-TCP Cerasorb™M
12	52	F	β-TCP Cerasorb™M

*M=Male, *F=Female

2.3 Clinical procedures

2.3.1 Radiographic examination

Routine panoramic radiographs were used for the assessment of all patients, pre-operatively, post-operatively and 6 months after SFA, to examine bone volume deficiencies and any pathological conditions in the augmented sinus floors. In addition, cone beam computed tomography (CBCT) (KaVo-3D- eXam®, KaVo Dental GmbH, Germany) was obtained in all cases for 3D evaluation of bone volume and anatomy of the sinus floor preoperatively.

2.3.2 SFA procedures

2.3.2.1 Pre-surgical preparation

Before augmentation surgery, all patients were prescribed oral prophylactic course of 1000 mg Amoxicillin (Ratiopharm®, Ulm, Germany) for 3 times daily or 600 mg Clindamycin (Ratiopharm®, Ulm, Germany) (3 x daily) in case of antibiotic hypersensitivity. These courses had to be continued 5-7 days of post-augmentation procedures to avoid infection. Analgesic medication to reduce pain and swelling such as 600 mg Ibuprofen for three days were optionally given to the patients under gastric-protection with 40 mg Pantoprazol-ratiopharm®.

2.3.2.2 SFA surgery

SFA was performed under local anaesthesia using a technique introduced by Tatum (Tatum, 1986). The average height of the residual alveolar crest was less than 4 mm. Therefore, a two-stage procedure was required to achieve initial mechanical stability of the inserted implants. The sinus floor was exposed by muco-periosteal incision, creating lateral access window to the maxillary sinus before preparing the Schneiderian membrane. This was followed by gently reflecting and elevating the underlying sinus membrane, creating adequate space for grafting the sinus floor. The reflection of sinus membrane should be in an apical direction and to the medial wall of the sinus to avoid pressure on the graft material and damage the membrane. The access windows in all patients were subsequently covered by synthetic collagen membranes (Colprotect®, Botiss, Germany). Finally, the flaps were repositioned and sutured. In all patients the healing period was six months between the first and second surgeries.

2.3.3 Dental implant surgery and biopsy specimen sampling

6-months post augmentation, dental implants placement and biopsies specimen removal were carried out under local anesthesia by the same surgeon. In each patient, a crestal incision with mesial relief, and a muco-periosteal flap was designed. Consequently, the assessment of the implantation sites was carried out (Figure 2-1). Bone biopsies specimens were sampled, and dental implants were inserted into the

augmented sites. Implant placement procedures were accomplished as previously described (Knabe *et al.*, 2008b).

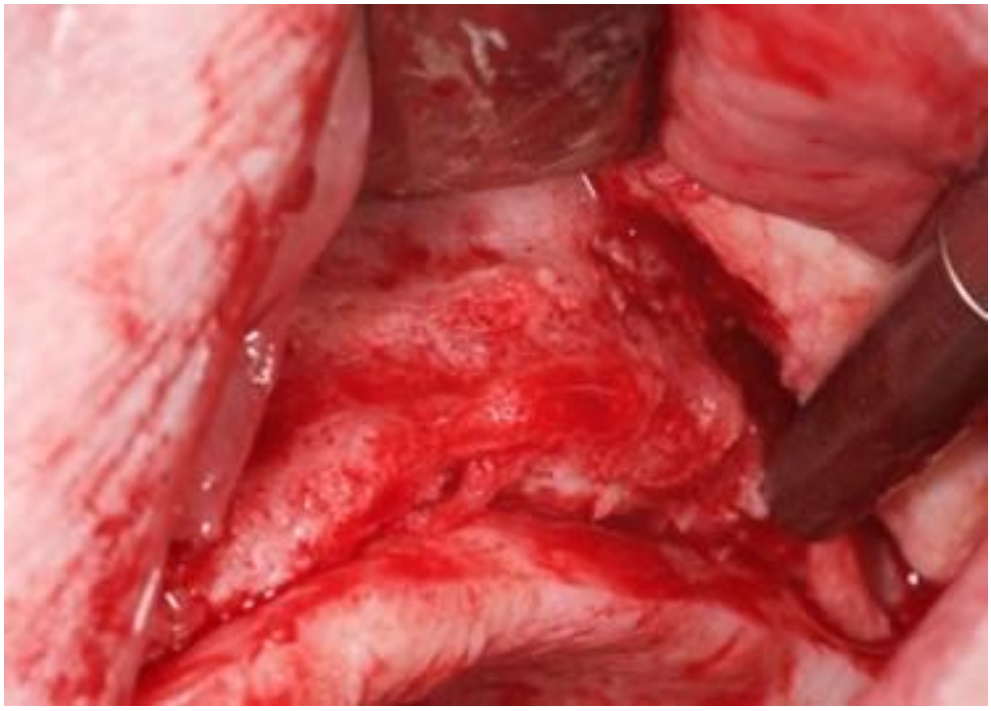

Figure 2-1: Intra-operative assessment of implant site

At the implant beds, one cylindrical bone biopsy was successfully harvested from each sinus with a trephine bur (Straumann GmbH, Freiburg, Germany) under cooling with isotonic saline solution, roughly 2.5 mm in diameter and 10-12 mm in length (Figure 2-2). The harvested samples were eventually used for histology, immunohistochemical, and histomorphometric analysis. The samples included both the native alveolar bone process and the augmented regions. The height of the native alveolar crest was about 1-3 mm for each biopsy and was not considered for the histomorphometric evaluation. After sampling specimens, the implant beds were prepared for implant insertion, and a total of 26 implants (Camlog, Straumann, Zimmer, or Ankylos) were inserted directly in 24 grafted sites followed by wound closure. The implants were allowed to heal for another 6 months until their exposure.

Figure 2-2: Biopsy specimen harvesting using a trephine drill. The inner diameter of the drill sets the diameter of the biopsy. The maximum length of the biopsy was approximately 10-12 mm.

2.4 Laboratory procedures

2.4.1 Specimen preparation technique

The specimens were processed used a reliable technique which facilitated carrying out the immunohistochemical analysis on resin embedded hard tissue sections as previously described (Knabe *et al.*, 2006). After the biopsy collection, the bone tissue samples were immersed in HistoChoice® fixative solution (Ref: H120 + H2901, Sigma-Aldrich, USA and Amresco Solon, OH, USA) at room temperature (20-22◦C) for five days to maintain tissue antigenicity and then processed for tissue histology as described in Table 2 - 4. The fixed samples were first dehydrated in acetone with 0.5 % v/v of poly-ethylene glycol-400 (PEG 400) for 5 days in a freezer (-20 ◦C) and then in acetone for 1 day at 4◦C, methyl benzoate for 2 × 5 days at 4◦C and Xylol for 1 day at 20-22◦C, respectively. This was followed by infiltrating the samples at 20-22◦C in a solution containing 8 ml methyl methacrylate (MMA), 12 ml *n*-butyl-methacrylate (BMA) and 0.4 ml PEG 400 for three days at a ratio of 40:60:2, respectively. After dehydration and infiltration, the embedding of the biopsies was performed in two stock solutions. Solution I consisted of 8 ml MMA and 160 mg benzoyl peroxide (BPO) catalyst, whereas solution II contained 12 ml BMA, 240 ml PEG 400, and 120 ml N,N-dimethyl-p-toluidine (DMT). Both solutions

were subsequently mixed in a ratio of 2:3 (solution I: solution II) and stored at 4◦C for at least 1 day.

After polymerizing the embedded samples in the mixture solution, the tissue blocks were removed from the polyethylene containers, fixed on the sample adapter using a 2 component-epoxy resin adhesive (Kulzer, Germany), consisting of Technovit® 3040 and Technovit® Universal Liquid. For the sectioning, the blocks had to be placed on the block holder and the cutting process was adjusted by adding the thickness of the samples (30 µm) to the thickness of the saw blade (350 µm) to become 380 µm. 50 µm-sections were cut parallel to the long axis of the biopsies using a 1600 Leitz sawing microtome (Leitz, Germany), under cooling tap water and then glued to plexiglas acrylic slides (patho-service GmbH, Germany) for 30 min. using a 2 component epoxy resin adhesive system (UHU GmbH, Bühl, Germany) at a ratio of 1:1. Finally, the sections had to be ground and polished using 1200 and 4000 grit wet silicon carbide paper (Exakt 400 CS, Exakt, Germany).

Table 2-4: Histological tissue technique

Histological Tissue Procedures	Solutions	Time + Temperature	Resources
1. Fixation	HistoChoice®	5 days, 20-22◦C	• Sigma-Aldrich, USA Ref:H120+H2901 • Amresco®, Solon, USA
2. Dehydration	Acetone + PEG 400 Acetone Methyl benzoate Xylol	5 days, -20◦C 1 day, 4◦C 5 days, 4◦C 1 day, 20-22◦C	• Merck KGaA, Germany • Merck, Germany • Merck, Germany • AnalaR Normapur, VWR Problao Chemicals, France.
3. Infiltration	PEG400 + MMA + BMA	8 days 20-22◦C	• Merck KGaA, Germany

4. Embedding	-Solution I: MMA + BPO -Solution II: BMA+ PEG 400 + DMT	1 day, 4°C	• Merck KGaA, Germany
5. Polymerization	Technovit 3040 Technovit-Universal Liquid	1 day ,4°C	• Kulzer, Germany

2.4.2 Histology and immunohistochemistry technique

A hard tissue histologic technique was used, which reliably allows performing immunohistochemical analysis on sawed sections of bone containing BSM (Knabe *et al.*, 2006). This technique was used for identification and visualization of protein expression, and specific tissue and cellular components utilizing labelled antibodies that can provide quantitative and qualitative data on tissue formation. The deacrylated sections were stained immunohistochemically using primary mouse monoclonal antibodies particular to osteocalcin (OC) and alkaline phosphatase (ALP), whereas rabbit polyclonal antibodies were particularly used to bone sialoprotein (BSP), collagen type I (Col I) and von Willebrand factor (vWF).

Before the immunohistochemical staining process, the sections were deacrylated by immersing in three different solutions; 2 × 20 min toluene (Ref: 1-083232500, Merck, Germany), 2 × 20 min xylene (VWR, France) and 1 × 10 min acetone, respectively. The samples were rinsed with distilled water and then stored in the pre-prepared TRIS buffer consisting of 1.8 g TRIS-Base, 13.2g TRIS-HCl (Merck, Germany) and 17.56 g NaCl (Merck, Germany) with 2 litres distilled water at pH 7.4. They were subsequently stored in Tris buffer in the freezer overnight. The sections were dried and surrounded with a DAKO Pen (Ref: S2002, Dako, Germany). To prevent nonspecific reactions, the samples were incubated with 2% bovine serum albumin (BSA) (Ref: 7030, Sigma, St. Louis, USA) in DAKO antibody diluent (Ref: S2022, DAKO, Germany) for 20 min and re-rinsed 3 × 20 min with Tris buffer for inhibiting non-specific binding sites. The activity of endogenous peroxidase was inhibited by incubating the specimens in Peroxidase Enzyme Blocking

Solution (Ref: S 2003, Dako, Germany) for 10 min (20-22°C), following by 3 × 2 min rinse with Tris buffer. Subsequently, the primary antibodies were diluted in DAKO Antibody Diluent for 30 min. The antibody solution was applied to the sections for binding to the proteins (100 µl per section). The dilution of primary antibodies was carried out according to Table 2-5.

Table 2-5: Primary antibodies used for immunohistochemical staining

Antigen	Isotype/Origin	Clonality	Dilution	Resource
OC	IgG3 Mouse	OCG3 Monoclonal	1:200	Abcam, U.K Ab 13420
Col I	Rabbit	Polyclonal	1:200	NIDCR, Dr. Larry Fisher, Maryland, USA LF-39
BSP	Rabbit	Polyclonal	1:200	NIDCR, Dr. Larry Fisher, Maryland, USA LF-84
ALP	IgG2a Mouse	8B6 Monoclonal	1:500	Sigma, U.S.A A2951
vWF	Rabbit	Polyclonal	1:700	Abcam, U.K Ab6994

The immunohistochemical staining was carried out using primary mouse monoclonal antibodies to OC and ALP, whereas rabbit polyclonal antibodies were particularly against BSP, Col I and vWF. Negative controls included mouse and rabbit primary antibodies were applied (PP54 and PP64) (Millipore, Billerica, Massachusetts, USA). This should reveal nonspecific binding of the primary and secondary antibodies to human tissues. Thus, false positive results were ruled out. The dilution of the mouse and rabbit antibodies was 1: 12500 and 1: 5250, respectively. Rinsing was repeated for 3 × 2 min with Tris buffer and followed by incubating the samples with secondary antibodies, peroxidase-labelled polymer and conjugating with goat anti-mouse and anti-rabbit antibodies using DAKO EnVision™ + Dual Link System-HRP (Ref: K4063, Hamburg, Germany) (Table 2-6). This was followed by 3 x 2 min washes with Tris buffer.

The color was developed by a peroxidase reaction, which is capable of oxidizing a colorless chromogen to a colored product. The chromogen color was developed by adding AEC System + Substrate Solution (Ref: K3461, Dako, Hamburg, Germany) for 10 min. After that, a red product was produced. This allowed the antigen-antibody compound to be visualized by a light microscopy. The samples were rinsed 3 x 2 min with distilled water. This was followed by counterstaining with Mayer's Hematoxylin (Merck, Germany) for at least 1 min and subsequent addition of tap water for 2 min and then rinsing with distilled water, resulting in a purple or blue colour. Finally, the slides had to be covered with coverslips (24 x 32 mm, Thermo-Scientific, Germany) using Kaiser's glycerine gelatine at 50°C (Ref: 1.09242.0100, Merck, Germany) and followed by using Fixogum (Marabu, Germany) for several hours to avoid air bubbles. The slides were ready for examination under light microscope to detect positively stained cells and tissue matrix components.

Table 2-6: Secondary antibodies used for immunohistochemical staining

Antigen	Origin	Conjugation	Resource
Mouse Rabbit	Goat	Peroxidase labelled polymer	DAKO, Germany K4063

Additional sections were stained for tartrate resistant alkaline phosphatase (TRAP) to identify osteoclast activity using a prefabricated Leukocyte Kit (Sigma, USA) based on the method described by Goldberg and Barka (Goldberg and Barka, 1962).

The slides were stored in Tris buffer at 37°C, and the distilled water had to be prewarmed to 37°C before to use. Firstly, the fixative solution from the "Acid Phosphatase" Leukocyte Kit (Protocol Nr. 387, Sigma-Aldrich, USA) was prepared and then warmed to 18–26 °C. Secondly, the slides were fixed by incubating in the previous solution for 30 sec. and then rinsing thoroughly in deionized water. The slides had to keep moist. Thirdly, a mixture of 0.5 ml Fast Garnet GBC Standard Solution with 0.5 ml Sodium Nitrite Solution (Ref: 914) from the previous kit were prepared for 30 sec. and left standing for at least 2 min. Subsequently, a mixed solution of pre-warmed 45 ml

deionized water (37°C), 1 ml Diazotized Fast Garnet GBC solution from the third step, 0.5 ml Naphthol AS-BI Phosphate Solution, 2 ml Acetate Solution and 1 ml Tartrate Solution were added respectively in a suitable jar (37°C) in a water bath. The incubation of the slides was then performed for 1 hour in 37°C water bath and needed to protect from light. Finally, the slides were thoroughly rinsed with deionized water before counterstaining for 2 min in Mayer's Haematoxylin Solution. Subsequently, the slides were ready for the microscopic evaluation. The positive controls containing osteoclasts were obtained from fracture healing sites as mentioned previously (Knabe *et al.*, 2008b, 2017c).

2.4.3 Histomorphometry

The histomorphometric assessment of the biopsies was carried out on a pair of sections 150 µm apart. All sections were imaged using a BX 63 light microscope combined with a DP 73 digital camera and cellSens Imaging Software System (Olympus, Hamburg, Germany) for recording as previously described (Knabe *et al.*, 2008b, 2017b). The overview multialigned MIA images of the individual biopsies were acquired using 10-x objectives. This was followed by selecting the regions of interest (ROIs) and processing for histomorphometric measurements. In each biopsy, two areas of interest were selected. The central area represents the centre of the augmented biopsy (ROI1) and the apical area represents the augmented area close to the Schneiderian membrane (ROI2) (Figure 2-3). ROI1 and ROI2 are of particular interest because in SFA, bone formation progresses from the crestal area towards the Schneiderian membrane in an apical direction. However, the crestal area (containing the native residual bone) was not included in this measurement.

A rectangular area of approximately 4 mm^2 in size (2 mm in width and 2 mm in length) was determined in both central (ROI 1) and apical areas (ROI 2) of each section. This was followed by measuring semi-automatically the surface area of newly formed bone and the surface area of the remaining particles in each ROI in each patient of both test groups, and then the data were separately calculated as a percentage of the total ROI area in both regions, and eventually, the data were expressed as mean ± SD in both regions for each group.

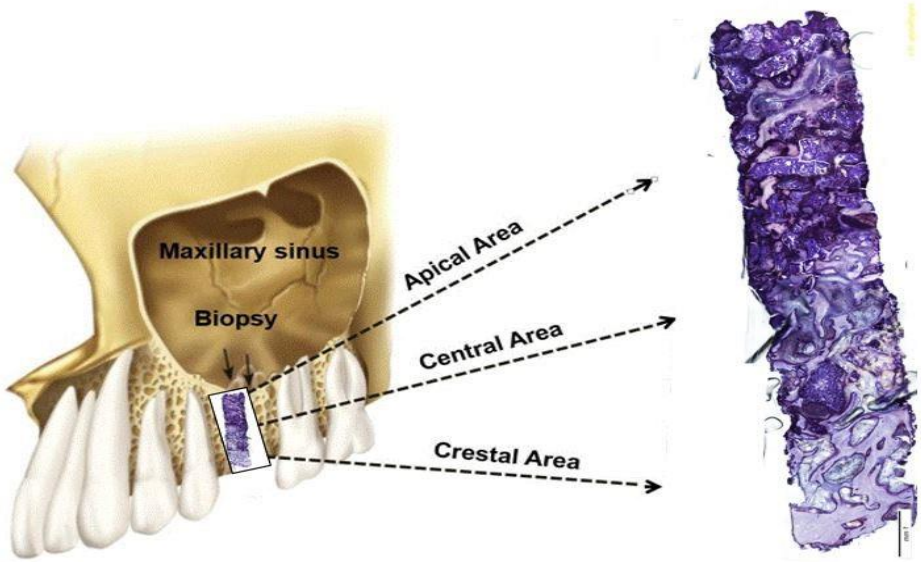

Figure 2-3: Schematic diagram showing the image of a biopsy sampled 6 months after SFA.

2.4.4 Immunohistochemistry analysis and immunoscoring system

The immunohistochemically-stained sections were analyzed semi-quantitatively regarding the intensity of the staining in each tissue component observed under the light microscope. The cell and tissue matrix components in both regions were histologically identified on morphological ground and examined for antibody decoration. Cellular components include osteoblasts, osteocytes and mesenchymal cells, whereas tissue matrix components include fibrous matrix, osteoid and bone trabeculae (Knabe *et al.*, 2008b). For the immunohistochemical assessment, the same ROIs were used as for the histomorphometric measurements.

Immunoscoring system was used to quantify the degree of immunohistochemical staining for the osteogenic markers in each cell and matrix component observed under the microscope. A score was assigned depending on whether the staining was mild, moderate or strong, it was also assessed whether the staining was localized or generalized in both areas. A score of "+++" [=4], "++" [=3], and "+" [=1] corresponded to localized strong, moderate and mild staining, whereas a score of "+++" [=5], "++"

[=4], and "+" [=2] correlated to generalized strong, moderate or mild staining. A score of (0) assigned to no staining (Table 2-7).

Table 2-7: Immunoscoring system was applied

Localization	Level of expression	Rate of Intensity	Scoring Number
Localized	Strong	+++	4
	Moderate	++	3
	Mild	+	1
Generalized	Strong	+++	5
	Moderate	++	4
	Mild	+	2
	No expression	0	0

Subsequently, the average scores for the degree of staining of these components for each particular marker were calculated in both ROI 1 and ROI 2 of 24 patients grafted with Si-CAOP and β-TCP, respectively. An average score of 3.5-5 for a given marker in a given cellular or tissue component was assessed as strong expression, while an average score of 2.3-3.4, 1-2.2 and 0.1-0.9 was categorized as moderate, mild and minimal expression, as previously described (Knabe *et al.*, 2008b, 2017b).

2.5 Statistical analysis

The histomorphometric and immunohistochemical data were presented as mean ± standard deviation (SD). Statistical analysis was carried out using the *Mann-Whitney-U Test* and OriginPro Software (2016; version 9.3) for comparing the two test groups. A value of $p \leq 0.05$ was considered statistically significant.

3. Results

3.1 Clinical results

6 months after unilateral SFA with Si-CAOP or β-TCP particles, none of the selected patients showed any postoperative complications such as sinusitis or Schneiderian membrane perforations. Normal wound healing was observed after primary and secondary surgeries. Although one sinus (patient no. 1) with Si-CAOP implantation illustrated thickening of the Schneiderian membrane, it clinically demonstrated to have good bone repair and regeneration. According to the oral surgeon, there were differences in the drilling characteristics noted between the two test groups in the implant regions. When preparing the implant sites, the Si-CAOP group exhibited more homogenous mature bone tissues with superior drilling resistance, when compared to the β-TCP group.

Six months after grafting of the sinus floors, all patients displayed a sufficient bone volume for implant placement, with satisfactory primary stability. 26 dental implants were successfully inserted in 24 grafted sinuses, and no implant failure occurred in both patient groups during the research period. The retrieved biopsies varied slightly in their length and exhibited healthy bone structures on a macroscopic level.

3.2 Radiological results

The panoramic radiographs of the grafted sites were taken in all cases. The imaging showed a marked degree of particle resorption after 6 months of augmentation. In sites grafted with Si-CAOP, the tissue in the grafted area displayed to a greater extent the appearance of cancellous maxillary bone with a lower degree of residual graft materials when compared to sites grafted with β-TCP. In both patient groups, there were no pathological conditions of the augmented sinuses, the Schneiderian membrane, or the adjacent tissues postoperatively, 6 months after SFA and after implant placement.

3.3 Histology, histomorphometry and immunohistochemical results

3.3.1 Results of histology and histomorphometry analysis

The histological examination of the hard tissue sections was carried out in both patient groups. The stained sections exhibited new bone formation, matrix mineralization, and partial resorption of the graft material in both the central and apical areas with the exception of one biopsy grafted with Si-CAOP (patient no. 4), which showed complete resorption of the Si-CAOP particles being completely replaced with fully regenerated bone tissue.

It was easy to differentiate between the morphology of both particles. For example, the residual Si-CAOP particles were present as achromatic rounded islands containing highly variable crystalline structures with large size, which was surrounded by a large amount of regenerated cancellous bony trabeculae (Figure 3-1 (A)), whereas the remaining β-TCP particles appeared as small grape-shaped clusters containing spherical or polygonal particles embedded within the newly osseous tissue (Figure 3-1 (B)). The new bone deposition was evident at the surface of the highly degraded residual Si-CAOP (Figure 3-1 (A)) or within the residual β-TCP, resulting in partial embedding of the TCP particles in the new mineralized bone tissue (Figure 3-1 (B)). No incidence of inflammatory reactions was seen in any of the augmented sites 6 months after SFA (Figure 3-1 (A, B)). The ratio between the newly formed bone and particles was relatively different in the grafted sinus floors based on the type of BSM and area of interest. Good bone-bonding properties were observed, and bone formation was preceded by enhanced proliferation and differentiation of osteoprogenitor cells in the mesenchymal tissue, with positive osteogenic marker expression for OC, Col I, BSP and ALP in the bone tissue elements. This was indicative of continuing matrix mineralization and bone formation.

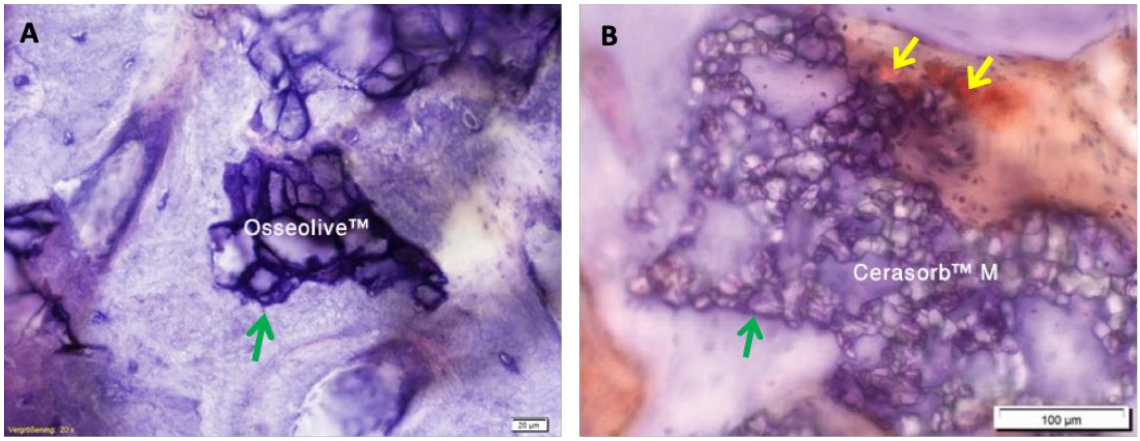

Figure 3-1: Histomicrographs showing the morphological appearance of the residual Ossolive™ (Si-CAOP) or Cerasorb™ M (β-TCP) particles in the human biopsies immunohistochemically stained and counterstained with hematoxylin 6 months after SFA. (A) Histochemical detection of OC in the central area of biopsy sampled after grafting with Si-CAOP (patient no. 11) shows a chromatic small and rounded island of particles containing crystalline like structures surrounded by the newly formed mature bone trabecula, with active bone remodeling and integration. A higher tendency for the residual Si-CAOP particles to degrade and being completely embedded in the newly formed bony trabecula with direct bone-particle contact (green arrow) is present (bar=20 µm). **(B)** Deacrylated section of biopsy sampled after grafting with β-TCP and stained for BSP exhibits small and irregular clusters of polygonal particles with lower tendency to disintegrate and formation of bony islands within their interconnecting pores. Strong staining of cells and non-mineralized osteogenic mesenchyme (yellow arrows) is present. The direct contact between bone-forming cells and the particles is evident (green arrows) (bar=100 µm).

For the histomorphometric analysis, a rectangular area of roughly 4.0 mm^2 in size was defined centrally and apically in each section. The central ROI was located at a distance of approximately 3 mm from the native alveolar crest extending in an apical direction. The results of the histomorphometric analysis are given in Table 3-1 and show the bone area fraction and particle area fraction in both patient groups.

Table 3-1: Results of the histomorphometric analysis in each patient of the Si-CAOP (Osseolive™) and the TCP (Cerasorb™) M groups

Group (A)	Osseolive™-Central Area Fraction %		Osseolive™-Apical Area Fraction %	
	Bone	Particles	Bone	Particles
1	27.29	0.00	28.31	0.37
2	31.40	1.84	8.61	0.00
3	33.72	2.01	15.86	0.00
4	64.04	0.00	43.51	0.00
5	21.43	14.33	83.29	7.87
6	28.30	0.00	46.41	9,62
7	26.94	0.00	35.45	3.28
8	20.48	0.00	60.46	11.96
9	31.29	6.77	41.76	0.12
10	35.23	7.09	35.67	0.00
11	34.15	0.00	34.31	6.78
12	37.71	3.54	52.12	5.28
Group (B)	**Cerasorb™ M-Central Area Fraction %**		**Cerasorb™M-Apical Area Fraction %**	
	Bone	**Particles**	**Bone**	**Particles**
1	41.06	1.87	36.35	3.45
2	15.73	0.00	16.97	33.54
3	42.39	4.19	39.10	42.54
4	40.73	0.00	10.61	71.33
5	41.34	0.00	33.71	27.91
6	45.52	0.00	27.99	18.13
7	31.65	0.00	30.30	24.54
8	29.20	32.32	39.67	12.30
9	25.79	0.08	28.54	22.54
10	39.87	0.00	32.31	7.25

11	45.32	5.97	36,99	21.53
12	29.81	1.04	21.79	32.95

All values represent the percentage of new bone tissue area and residual particle area that was separately measured in both investigated regions for each patient of both groups.

Table 3-2: The final results of the histomorphometric analysis in both treatment Groups

Treatment Group	**Bone%**	**Particle%**
Osseolive™ central	32.6±11.19	2.9±4.4
Cerasorb™ M central	35.7±9.18	3.79±9.2
P-value	0.16	0.75
Treatment Group	**Bone %**	**Particle%**
Osseolive™ apical	40.48 ± 19.7	3.7±4.3
Cerasorb™ M apical	29.53±9	26.5±18
P-value	0.09	**0.000*** **

The bone area fraction and particle area fraction in each pair of section were analyzed (mean ±SD) as a percentage of the total group in each region. Asterisks (***) were used to indicate $P < .001$, which is statistically highly significant.

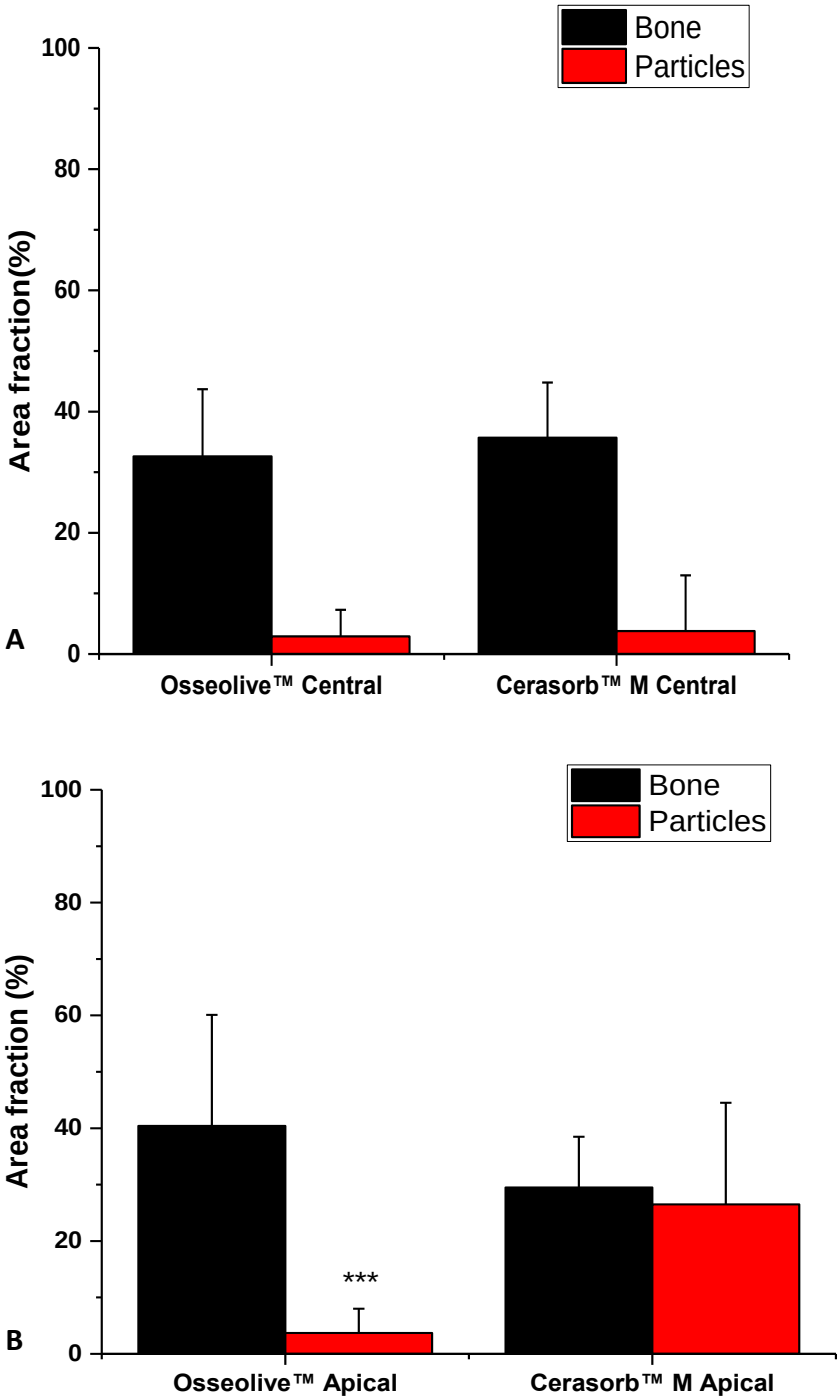

Figure 3-2: Histograms illustrating the results of histomorphometric analysis in the central and apical area of both groups. The area fraction of the newly regenerated bone and residual particles in the central **(A)** and apical **(B)** areas of 24 human biopsies augmented with either particulate Si-CAOP or β-TCP and sampled after 6 months of SFA is shown. All values represent mean ± SD (error bars) of two measurement parameters recorded in 12 patients. Asterisks in graph B show statistically highly significant differences in the residual particle degradation of patient group A (p <.001).

In the light of the above findings in Figure 3-2, in the central area of the samples, the mean bone area fraction (±SD) noted for the group A was 32.66 ± 11.19 %, and the mean particle area fraction was 2.9 ± 4.4%. This corresponded with a mean bone area fraction of 35.7 ± 9.18 % and a mean particle area fraction of 3.79 ± 9.2% in group B. In the β-TCP group, a slightly greater area fraction of bone and particles were recorded compared to the Si-CAOP group, as illustrated in Figure 3-2 (A). These differences were not statistically significant, though (p=0.2, p=0.7, respectively).

In the apical area of the Si-CAOP sites, the mean area fraction (±SD) of formed bone was 40.48 ± 19.7%, and the mean area fraction (±SD) of grafted material was 3.7 ± 4.3%, whereas in the β-TCP sites, the mean bone area fraction of 29.53 ± 9% and the mean material area fraction of 26.5 ± 18% were observed in Figure 3-2(B). Therefore, the Si-CAOP group displayed greater amount of bone formation in the apical area of the grafted sinuses compared to the β-TCP group, but the differences were not of statistical significance (p=0.09). This was associated with a significantly smaller amount of remaining Si-CAOP particles in the group A 6 months after SFA, with a highly significant difference in residual particle area were observed between group A to group B (p<.001). Furthermore, the amount of the newly formed bone was higher in the apical area of the Si-CAOP samples compared to their central areas, while in biopsies sampled with TCP, bone formation area was greater in the central area compared to the apical region (Figure 3-2 (A, B)).

It seems clear from the histological data that 6 months after SFA that in both Osseolive™ and Cerasorb™ M groups, new bone formation, and matrix mineralization had occurred with residual particles being embedded within the newly formed osseous tissue. However, the highly porous Si-CAOP material was able to induce greater bone formation in the apical area of the patient group A in combination with considerably greater particle degradation in both regions compared to the β-TCP material. In addition, the Si-CAOP Osseolive™ particles displayed high bone-particle contact (data not shown).

3.3.2 Results of immunohistochemical analysis of osteogenic marker expression

Positive immunohistochemical staining for all osteogenic proteins and enzymes was detected in the various cells and tissue components (osteoblasts, osteocytes, mesenchymal cell, fibrous matrix, osteoid and bone matrix), which had formed in the sites augmented either with Si-CAOP or β-TCP 6 months after augmentation. The immunohistochemical findings of the osteogenic marker expression analysis (OC, Col I, BSP and ALP) are illustrated in Table 3-3 (A-D). This table displays the mean values ± SD of the scores for the osteogenic marker expression in the bone tissue components in the biopsies sampled from the Si-CAOP patient group compared to biopsies harvested from the TCP patient group. Bone formation in both patient groups was accompanied by positive expression of OC, Col I, BSP and ALP in the cells and tissue matrix components in contact with the Si-CAOP or TCP particles.

The Si-CAOP particles were highly degraded and nearly completely replaced by newly formed bony trabeculae with direct bone-particle contact, as shown in Figure 3-4 (A). The highly degraded particle residues are embedded within these newly formed trabeculae, and osteoblasts, which strong staining for OC have migrated into the pores of these highly degraded particle residues and are in the process of laying down mineralizing bone matrix. This is indicative of good bone-bonding behavior with rapid particle degradation in 6 months healing time. Stronger OC staining and more enhanced expression in mineralized bone matrix were noted in the central area of the biopsies for both the Si-CAOP and β-TCP patient groups, as compared with mild positive staining in the apical area of the biopsies of each group, but the differences were not statistically different (Figure 3-3 (A, B)). This was accompanied by significantly greater OC staining of the osteoid in group A when compared to group B (p=0.01, centrally; p=0.002, apically). In the β-TCP biopsy specimens, significantly stronger OC expression in the unmineralized fibrous matrix was present in the central area, when compared to the Si-CAOP biopsies (p=0.002) (Table 3-3 (A), Figure 3-3(A, B)).

In the central area of the Si-CAOP patient group, more enhanced OC expression in osteocytes and mesenchymal cells was observed, when compared to the TCP patient group (Figure 3-3 (A, B)), while minimum expression of osteoblasts was noted in both

regions. Only one biopsy of the Si-CAOP group showed moderate localized OC expression in osteoblasts and the unmineralized fibrous matrix of the osteogenic mesenchyme in the apical area (Figure 3-4 (A)). In contrast, a higher tendency for OC staining was observed in osteoblasts of the β-TCP group, while only a few osteocytes showed positive OC staining (Figure 3-4 (B)), but no statistically significant differences were found (Figure 3-3(A, B)).

Table 3-3: The results of the immunoscoring of osteogenic marker expression in different cell and tissue components in the central and apical regions of the biopsies

(A) Osteocalcin Expression (Mean ± SD)						
GROUP	OB	OC	MC	FM	OS	B
Osseolive™ Central Cerasorb™M Central	0.3±1.2 0.9±1.7	0.8±1.5 0.4±0.9	0.4±1.2 0±0	0.3±0.5 2.1±1.5	1.6±1.9 0.2±0.6	2±1.9 1.8±1.7
p-value	0.31	0.56	0.15	**0.002****	**0.012***	0.86
Osseolive™ Apical Cerasorb™M Apical	0.3±1.2 1.3±1.9	0.3±1.2 0.4±0.9	0.8±1.5 0.3±1.2	1.2±1.3 1.9±1.7	1.7±1.8 0±0	1±1.8 1.1±1.7
p-value	0.14	0.62	0.31	0.26	**0.002****	0.83
(B) Collagen Type I Expression (Mean ± SD)						
Osseolive™ Central Cerasorb™M Central	0.3±1.2 2.8±1.9	1.9±2 1.7±2.1	0.3±0.9 2.4±2.2	1.5±1.6 3.4±1.7	2±1.7 0.4±0.8	0.3±1.2 1.3±1.9
P-value	**0.002****	0.79	**0.008****	**0.011***	**0.012***	0.15
Osseolive™ Apical Cerasorb™M Apical	1.1±1.6 3.2±1.8	0.9±1.5 1.3±2.1	0.1±0.3 2.6±2.4	1.9±1.5 3.75±1.7	1.7±1.5 0±0	0.3±0.9 1±1.9
p-value	**0.009****	0.78	**0.006****	**0.009****	**0.000*****	0.25
(C) Bone sialoprotein Expression (Mean ±SD)						
Osseolive™ Central Cerasorb™M Central	1±1.8 2.9±2.4	1.9±2.0 1.3±2.1	1.8±2.0 2.1±2.3	3.3±1.8 3.4±1.8	2.3±1.7 0±0	2.1±1.6 0.9±1.4
p-value	**0.02***	0.48	0.62	0.95	**0.000*****	0.06
Osseolive™ Apical Cerasorb™M Apical	1.3±1.9 2.8±2.5	1.3±1.7 1.3±2	1.3±1.8 2±2.2	2.3±2.0 3.9±1.5	2.1±1.9 0.3±0.9	0.9±1.7 1.3±1.9
p-value	0.06	0.95	0.41	0.44	**0.009****	0.92
(D) Alkaline phosphatase Expression (Mean ±SD)						
Osseolive™ Central Cerasorb™M Central	0.2±0.8 0±0	0.0±0.0 0±0	0.7±1.4 0.3±0.9	0.8±1.3 1.2±1.5	1.3±1.8 0±0	0.0±0.0 0.7±1.2
p-value	0.32	1.00	0.29	0.69	**0.015***	0.07

Osseolive™ Apical Cerasorb™M Apical	0.3±0.9 0±0	0.1±0.3 0±0	0.3±0.9 0±0	0.6±1.3 1.2±1.5	0.7±1.6 0±0	0.2±0.6 0.7±1.3
p-value	0.15	0.32	0.32	0.40	0.15	0.27

The mean of the scores ± SD of the marker expression in the various cellular and tissue components OB=osteoblasts; OC= osteocytes; MC=mesenchymal cells; FM=fibrous matrix; OS=osteoid; and B=bone). An average score of 3.5-5, 2.3-3.4 and 1-2.2 was assessed as strong, moderate and mild overall expression of a respective osteogenic marker in a given cellular and matrix component, while an average score of (0) correlated with no or minimal staining (0.1-0.9). All values represent mean ± SD of six measuring parameters and values of $p < 0.05$ were considered significant (bold print). The statistical significance is shown as asterisk; (*) indicates a significant p-value, (**) represent very significant and (***) indicates an extremely significant *p*-value.

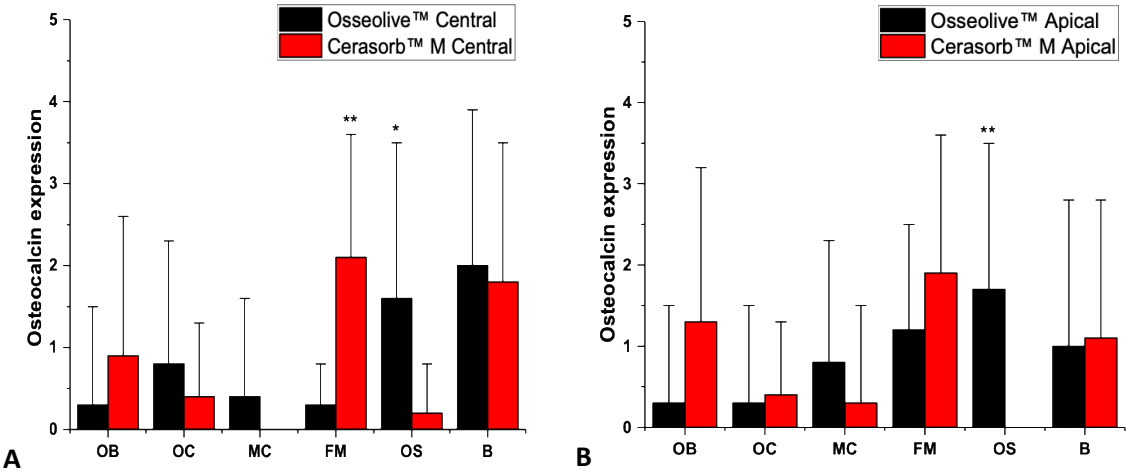

Figure 3-3: Histograms depicting the results of the OC marker expression in the central and apical areas of the biopsies of the Osseolive and Cerasorb M groups. Y axis represents the intensity of the marker in the cells and tissue components in each region for each group. **(A)** OC expression in the central area of the Osseolive™ and the Cerasorb™ M samples shows a significantly greater staining of unmineralized fibrous matrix in the Cerasorb™ M group than in the Si-CAOP group, associated with statistical significance; *p*=0.002**, whereas stronger staining of the osteoid for OC was noted in the Si-CAOP biopsies compared to the β-TCP biopsies. This was accompanied by significant *p*-value =0.01*. **(B)** The apical region of the Si-CAOP sites shows stronger OC expression in the osteoid, with statistical significance, *p*=0.002**, when compared to the TCP group.

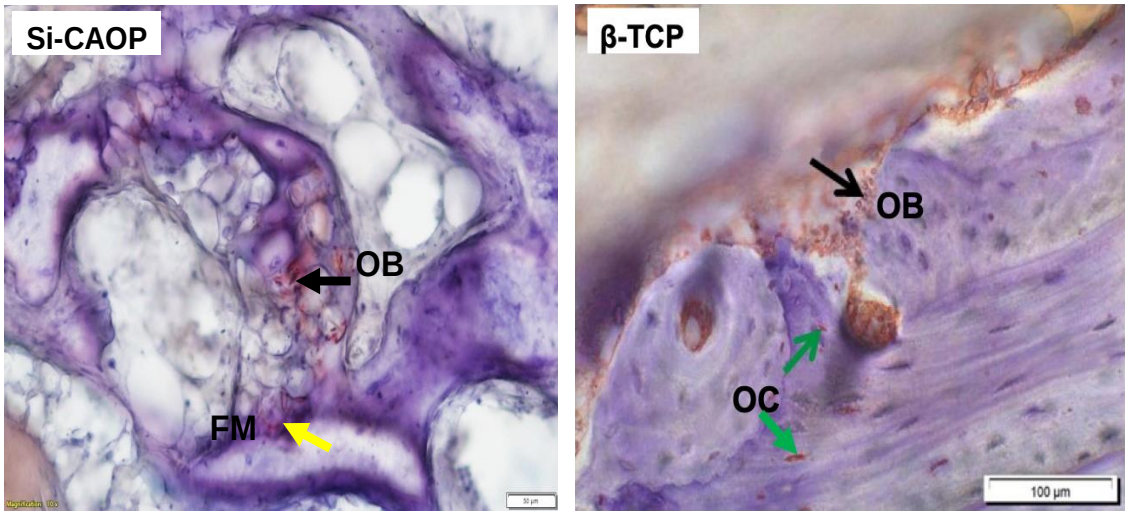

(A) **(B)**

Figure 3-4: Histomicrographs showing OC detection in deacrylated sections. Biopsies sampled 6 months after SFA with Osseolive™ or Cerasorb™ M particles, immunohistochemically stained for OC and counterstained with hematoxylin. **(A)** Histomicrograph of immunohistochemically stained section of the biopsy sampled after SFA with Si-CAOP (patient no. 3) shows highly degraded particles that are completely embedded in the newly formed bony trabeculae and display direct particle-bone contact. Moderate localized staining for OC is visible in osteoblasts (black arrow) and the not yet-mineralized bone matrix of the osteogenic mesenchyme (yellow arrow) in the apical area of the section (bar=20 µm). **(B)** A higher tendency for OC staining in osteoblasts (black arrow) lining the newly formed bone and positive staining of only a few osteocytes (green arrows) in the biopsy grafted with β-TCP (bar=100 µm).

In the Si-CAOP biopsies stained for Col I (Table 3-3 (B)), a mild expression with stronger staining of the osteoid surrounding the newly formed bone following 6 months' implantation was detected, when compared to the TCP biopsies (Figures 3-5 (C, D) and 3-6 (A)). These differences were significant in the central area (p=0.01) and extremely significant in the apical area (p<.001). Osteocytes displayed a mild expression of Col I centrally and therefore slightly greater staining compared to the β-TCP group. However, the Col I expression was at lower levels in the fibrous matrix of the osteogenic mesenchyme in the Si-CAOP biopsies, with the differences being statistically significant (Figure 3-5 (C)). In one section in group A (patient no. 12) a mild Col I expression in osteocytes and strong expression in the fibrous matrix were presented centrally (Figure

3-6 (B, C)), while in group B this marker was expressed strongly in osteoblasts (p=0.002, centrally; p=0.009, apically); mesenchymal cells (p=0.008, centrally; p=0.006, apically) and fibrous matrices of the osteogenic mesenchyme (p=0.01, centrally; p=0.009**, apically), when compared with the Si-CAOP samples (Figure 3-5 (C, D)).

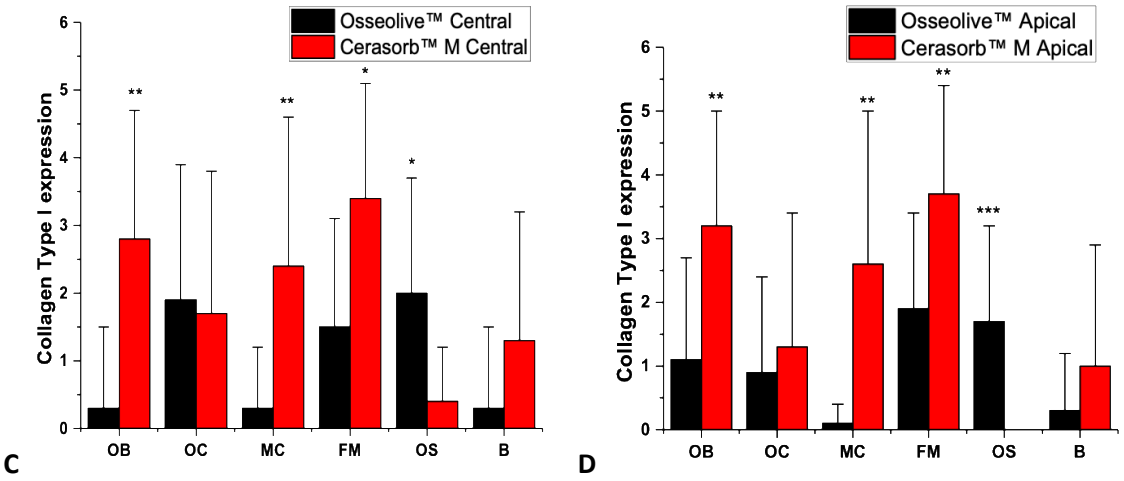

Figure 3-5: Histograms illustrating the results of the immunoscoring of the Col type I marker expression (mean values ± SD (error bars)) in the cells and tissue components formed in the both investigated regions. (C) The central area and **(D)** apical area of the Cerasorb™ M sites display stronger staining and expression of Col I in OB (p=0.002**, centrally; p=0.009**, apically), MC (p=0.008**, centrally; p=0.006**, apically), and FM (p= 0.011*, centrally; p=0.009**, apically) when compared to the Osseolive™ sites. There, however, was significantly greater Col I expression in the osteoid (OS) (p= 0.012*, centrally; p<.001***, apically) in the Si-CAOP biopsies than in the β-TCP biopsies.

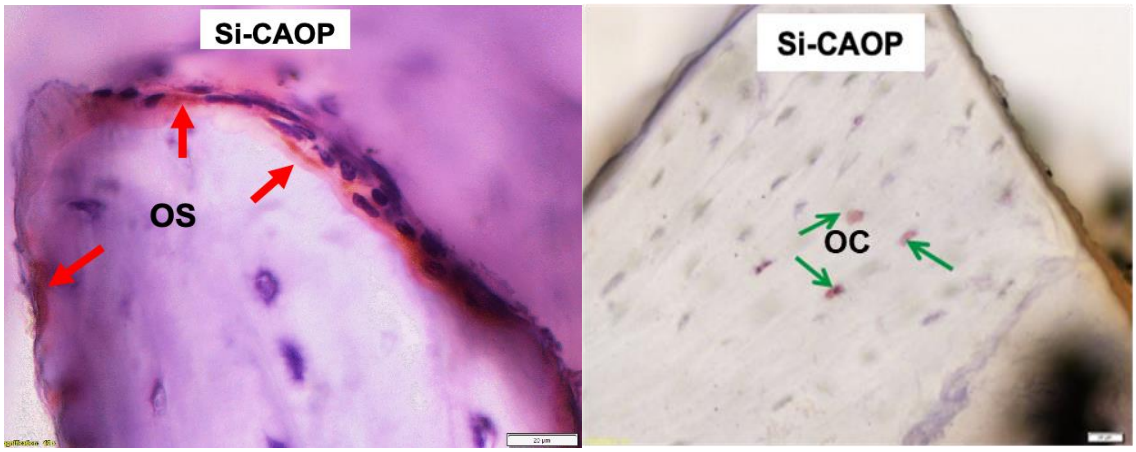

(A) **(B)**

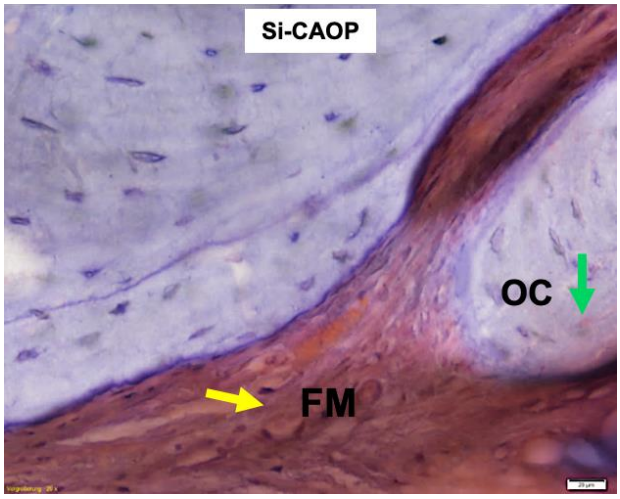

(C)

Figure 3-6: Histomicrographs of the Col type I detection after deacrylation. The biopsy was sampled after 6 months of implantation with Osseolive™ (Si-CAOP) particles stained immunohistochemically for Col I. **(A)** Histochemical detection of the Col I marker in a deacrylated sawed section stained for Col I augmented with Si-CAOP particles showed mild red staining of the osteoid (red arrows) lining the mineralized bony trabeculae in the central area of the biopsy (patient no. 4) (bar=20 µm). **(B)** Intense localized staining of active osteocytes (green arrows) for Col I in the central area of deacrylated biopsy (patient no. 12) sampled with Si-CAOP is visible (bar= 20 µm). **(C)** Immunodetection of Col I in deacrylated biopsy (patient no. 12) after 6 months sampled with Si-CAOP particles: strong expression in the fibrous matrix of the osteogenic mesenchyme (yellow arrow) and mild staining of osteocytes (green arrow) are present (bar=20 µm).

Positive expression of the BSP marker was clearly demonstrated in all cell and tissue components in both patient groups, as recorded in Table 3-3 (C). Compared to the Cerasorb™ M group, mild staining but higher expression of BSP was present centrally in the mineralized bone matrix of the Osseolive™ group with non-significant differences observed (p=0.06) (Figure 3-7 (E, F)). This was accompanied by mild to moderate BSP expression in the osteoid with very to extremely significant differences (p<.001, centrally; p=0.009, apically) (Figure 3-7 (E, F)). Although stronger BSP expression was noted in the unmineralized fibrous matrix of the osteogenic mesenchyme in the sites grafted with the β-TCP particles compared to moderate staining in the sites grafted with the Si-CAOP particles, the differences were not statistically significant (p=0.9, centrally; p=0.4, apically) (Figures 3-7 (E, F) and 3-9 (A, B)). However, in the patient no. 2, a strong generalized staining of the unmineralized fibrous matrix lining the osteoid and the newly formed bone tissue in the apical part was observed (Figure 3-8 (B, C)).

Furthermore, in the Si-CAOP group, higher BSP expression was noted centrally in osteocytes on the surface of the mineralized bone tissue than that in the other group without yielding statistically significant differences (Figure 3-7 (E)). However, a similar level of enhanced marker expression in positive osteocytes was observed in both groups, apically (Figure 3-7 (F)). Compared to group A, a higher, i.e. moderate BSP expression level was noted in osteoblasts of the TCP reference group with the differences being statistically significant in the central area; p=0.02 (Figures 3-7 (E) and 3-9 (A, B)). The immunoscoring data show a trend for higher expression of OC, Col I and BSP centrally in osteocytes of the Si-CAOP group, with these differences however not being statistically significant, as shown in Table 3-3 (A, B, C).

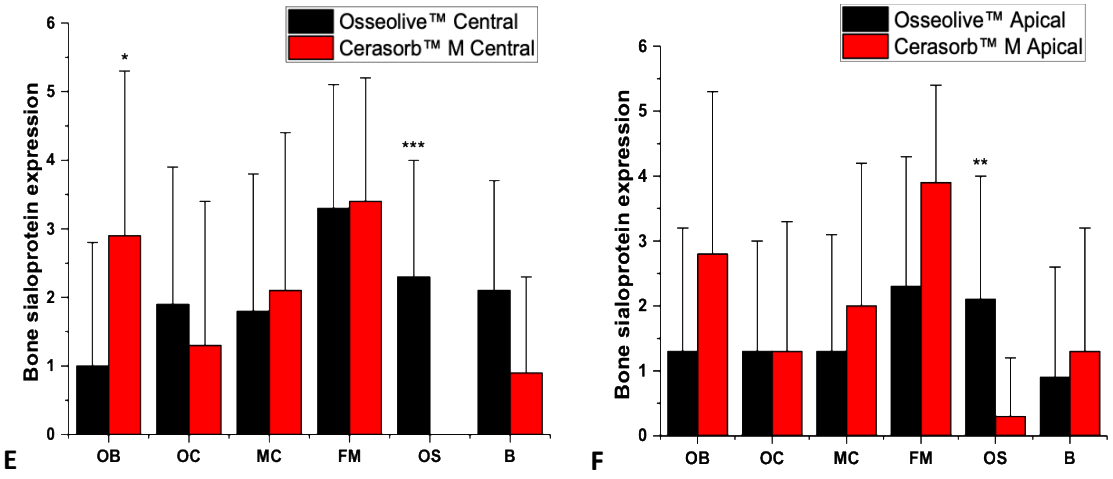

Figure 3-7: Histograms illustrating the mean values ± SD (error bars) of the immunoscoring for the BSP marker expression in the cell and tissue components formed in the sites augmented with Si-CAOP and β-TCP granules. Bone sialoprotein expression was strong in OB and FM centrally **(E)** and apically **(F)** in the Si-CAOP group, with these differences being statistically significant for OB centrally (p=0.02*), while the marker was much stronger expressed in OS in both regions for the Si-CAOP group than the β-TCP group with this difference being statistically significant (p <.001***, centrally; p= 0.009**apically).

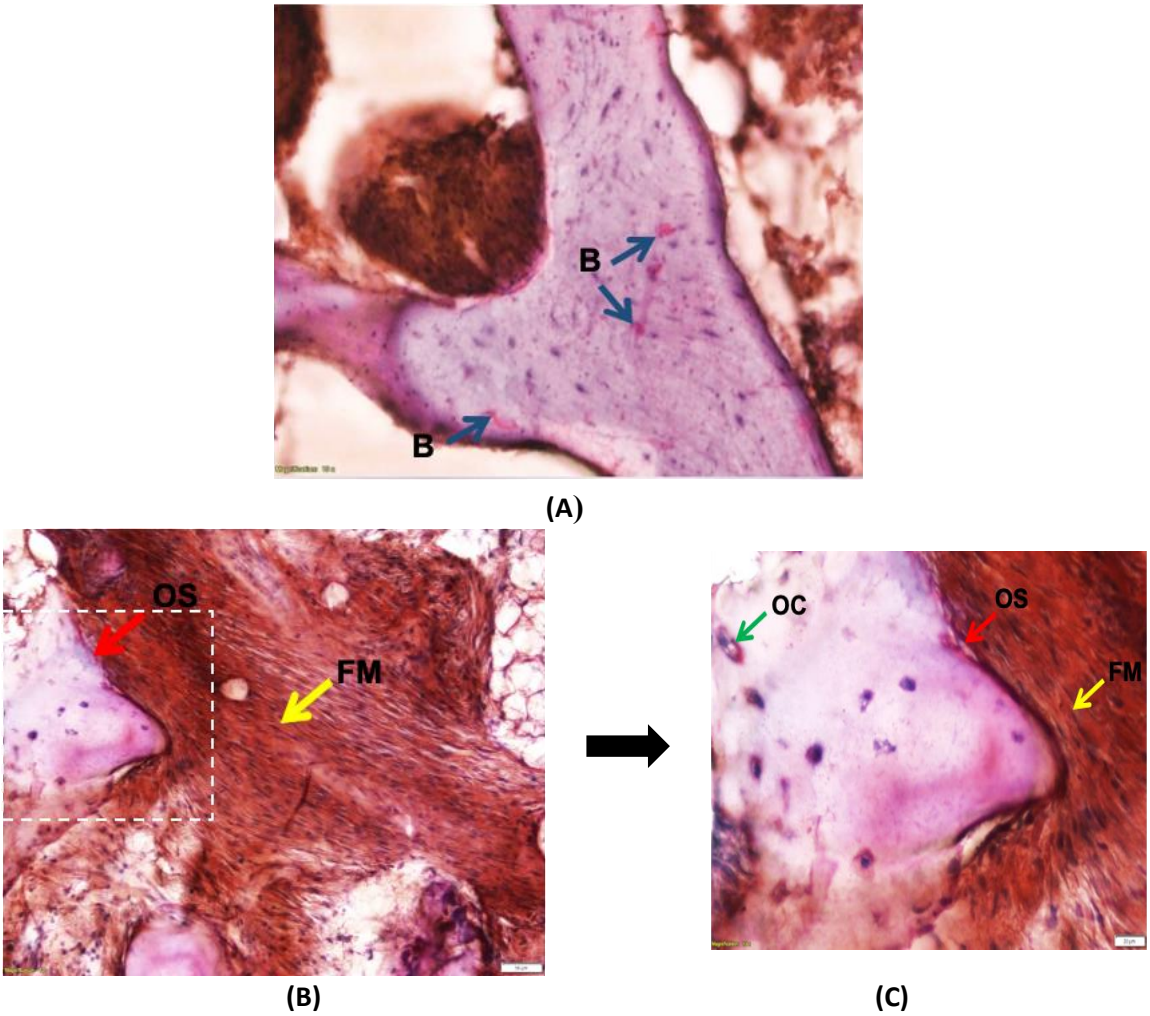

Figure 3-8: Immunohistochemical detection of BSP marker expression in human biopsies sampled 6 months after augmentation with Si-CAOP particles. **(A)** A deacrylated sawed section (patient no. 3) of biopsy grafted with Si-CAOP particles shows a mild localized staining of the mineralized bone tissue (blue arrows) displaying good bone regeneration in the central area. **(B)** A biopsy (patient no. 2) grafted with Si-CAOP particles exhibits strong generalized staining of the unmineralized fibrous mesenchymal matrix (yellow arrows) and mild to moderate localized staining of the osteoid (red arrows) lining the newly formed bone tissue in the apical region (bar=50 µm). **(C)** Enlargement of Fig. B. mild localized staining of active osteocytes (green arrow) in the regenerated bone tissue was present (bar=20 µm).

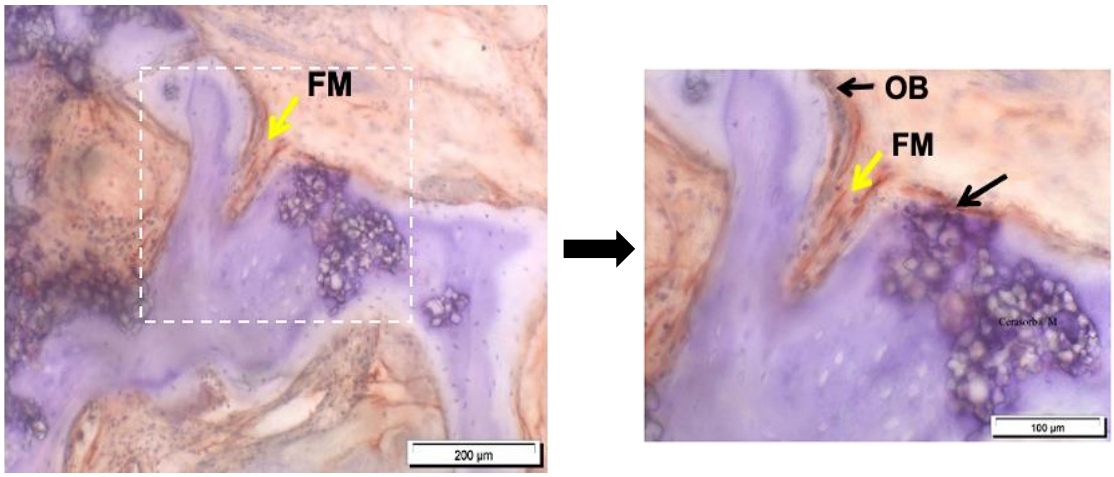

(A) **(B)**

Figure 3-9: Immunohistochemical detection of BSP marker expression in human biopsy sampled 6 months after augmentation with the TCP particles. (A) A deacrylated section stained for BSP shows that the β-TCP particles are not completely degraded and replaced by new osseous tissue in the central area of the biopsy. However, they display good osseous integration of the biomaterial with good bone bonding properties. Strong expression of BSP in cells and the unmineralized fibrous matrix of the osteogenic mesenchyme (yellow arrows) in contact with the β-TCP particles is particularly evident in the vicinity of osteoblasts (bar=200 µm). **(B)** Higher magnification of Fig. A displays moderate staining of a chain of osteoblasts (black arrows) lining the formed bone tissue (bar=100 µm).

In the Osseolive™ group, ALP showed mild expression and thus stronger staining in the osteoid compared with no staining recorded in the Cerasorb ™ group. This difference was statistically significant in the central area (p=0.01) (Figure 3-10 (G)). However, this was associated with mild and stronger staining of fibrous matrix of osteogenic mesenchyme in the second group compared to the first group (Figure 3-10 (G, H)). There furthermore was weak positive staining in osteoblasts and mesenchymal cells in the Si-CAOP sites (Figure 3-11) compared to no staining in the TCP sites without these differences being statistically significant (Figure 3-10 (G, H)).

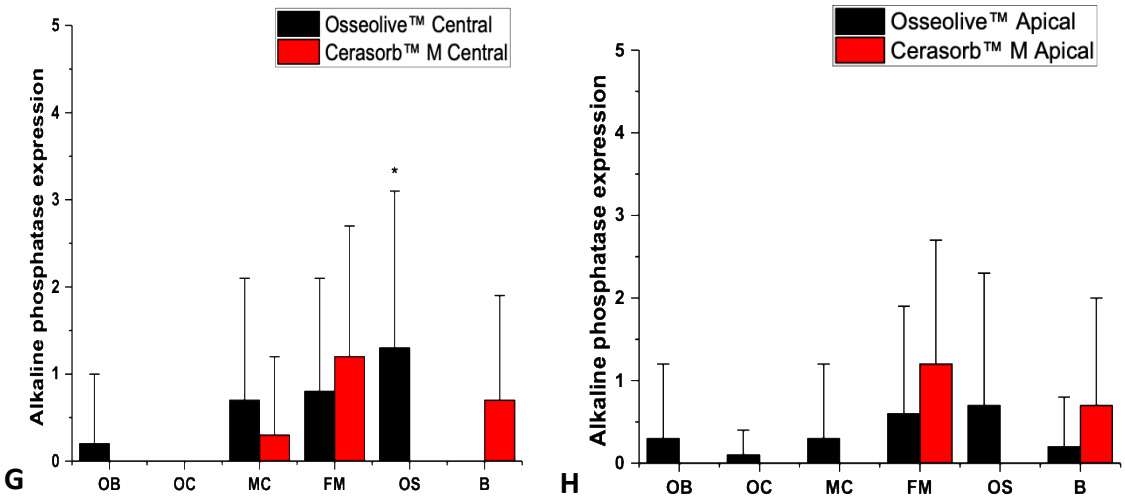

Figure 3-10: Histograms illustrating the mean values ± SD (error bars) of the immunoscoring for ALP marker expression in the cells and tissue components formed in the sites augmented with Si-CAOP and β-TCP particles. **(G)** ALP is more strongly expressed by MC in the β-TCP specimens, with no statistical significance (p=0.2), whereas it is highly expressed by OS in the Si-CAOP specimens, with a significant *p* value= 0.015 (typically p≤0.05).

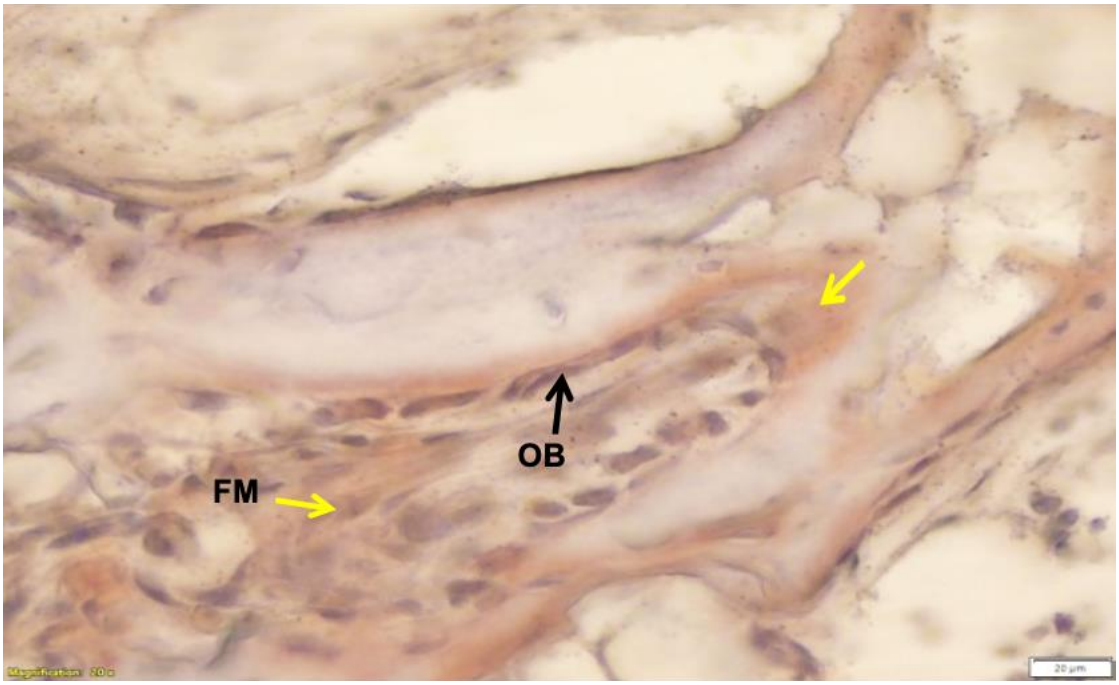

Figure 3-11: Immunodetection of ALP marker expression in the human biopsy 6 months after augmentation with the Si-CAOP particles. The patient biopsy (patient no. 3) shows mild localized staining of the osteoblasts (black arrow) and mild generalized staining of the unmineralized fibrous matrix of the osteogenic mesenchyme (yellow arrows) in the apical area (bar = 20 µm).

The positive expression of the osteogenic proteins and enzyme indicates that with both BSMs bone matrix synthesis and matrix mineralization, and therefore bone regeneration was still actively continuing 6 months after SFA, with a higher activity being present in the central region in the samples compared to the apical region. The most relevant finding is there was a tendency for significantly greater staining for OC, Col I, BSP and ALP in the osteoid of the Si-CAOP group than in the β-TCP group, while significantly higher expression of osteoblasts and unmineralized fibrous matrix for OC, BSP, and Col I was noted in the β-TCP group compared to the Si-CAOP group. This was in addition to higher OC, Col I and BSP expression in osteocytes in the Si-CAOP samples, whereas there was weak staining for ALP marker in osteocytes.

All sections stained for non-immunized rabbit and mouse IgG were negative. In the Si-CAOP samples stained for TRAP activity, no positive osteoclastic activity was found in osseous tissue surrounding the highly degraded Si-CAOP particles.

In summary, the findings of our study revealed a tendency toward higher bone formation and greater osteogenic marker expressions for OC, Col I, BSP and ALP in the osteoid and also partially in osteocytes and the mineralized bone matrix in the Si-CAOP group compared to the TCP group, being indicative more advanced bone formation.

3.3.3 Detection of angiogenic marker expression in biopsies augmented with the Si-CAOP material

Immunohistochemical staining of sections with the angiogenic vWF marker was used to detect new blood vessels formation in the vicinity of the Si-CAOP particles during bony integration, in the same rectangular area used for histomorphometry analysis. Under lower magnification, neovascularization in the porous structure of the Si-CAOP particles was visible at 6 months after augmentation, as shown in Figure 3-12. This finding revealed for the first time that angiogenesis was induced by the Si-CAOP particles in humans and seems to indicate that the Si-CAOP materials have the potential to enhance blood vessel formation during new bone formation. This was a pilot proof-of-concept

experiment, which examined the stimulatory effect of the Si-CAOP particles on angiogenesis in the posterior maxilla of four patients.

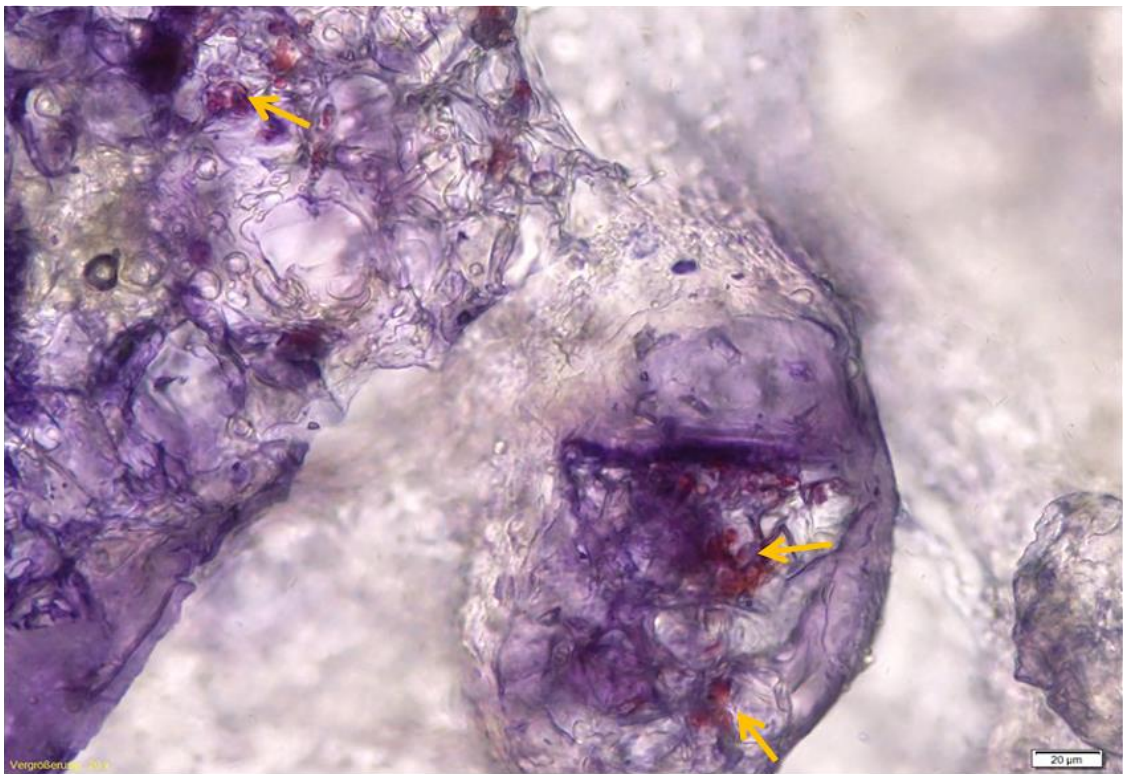

Figure 3-12: Immunodetection of vWF after deacrylation in the Si-CAOP biopsy. A 5-µm section was immunohistochemically stained for vWF and counterstained with hematoxylin. Histomicrograph showing capillary formation in the osseous tissue which formed in the pores of the degrading Si-CAOP Osseolive ™ particles (orange arrows) 6 months after SFA in the apical area of biopsy (patient no. 4) (bar=20 µm).

4. Discussion

Over recent years, the replacement of lost teeth with dental implants has become an increasingly common therapeutic approach in prosthodontic therapy. However, the bone resorption process after tooth extraction and the principle of restoration-driven implant placement often demand site management, before implants can be placed in the position required for a proper design of the implant-supported prosthesis. This means that bone regenerative procedures are often needed prior to the insertion of implants. On this basis, SFA first with autografts and then using tricalcium phosphate bone grafting materials has become a well-established pre-implantology surgical technique for ARA in the posterior maxilla (Knabe *et al.*, 2017b). In modern oral implantology, the use of resorbable synthetic bone substitutes to regenerate bone in the sinus floor has become an increasingly common practice, helping to avoid second-site surgery for autogenous bone harvest and the associated donor-site morbidity (Wheeler, 1997; Zerbo *et al.*, 2005; Aghaloo and Moy, 2007; Knabe, Ducheyne and Stiller, 2011; Knabe *et al.*, 2017c).

The application of biodegradable and bioactive CaP ceramics has been widely documented showing that these materials would simplify SFA procedures and enhance bone biosynthesis in preparation for dental implant placement (Wheeler, 1997; Knabe *et al.*, 2004b, 2008a, 2008b; Stiller *et al.*, 2014; Knabe *et al.*, 2017d; Starch-Jensen and Jensen, 2017). For ARA applications, bioactive CaP ceramics should be bone-bonding, although the rate of bone formed depends on the different types of ceramics used (Knabe *et al.*, 2004a). Ideally, they should activate bone formation at their surfaces, which combined with a high degradation rate as well as should result in bone defect regeneration and substitution by completely functional osseous tissue (Wheeler, 1997). In the sequence of events leading up to bone formation, this requires the capability of inducing osteoprogenitor cell differentiation including the expression of the osteoblast phenotype (Ducheyne and Qiu, 1999; Knabe *et al.*, 2004b). β-TCPs have been successfully implanted in humans, facilitating the deposition of the bone matrix within the pores of TCP particles in histological observations (Zerbo *et al.*, 2004; Knabe *et al.*, 2008b, 2017c). Therefore, they are regarded as alternatives to the use of autografts, which have been considered as the gold standard (Knabe *et al.*, 2008b; Stiller *et al.*,

2014). Although such particles have exhibited incomplete resorption (Zerbo *et al.*, 2004), they have displayed a greater degree of biodegradability than a bovine-derived HA material (Bio-Oss) (Cordaro *et al.*, 2008). Despite in-depth research on CaP materials since the early 1970s, the underlying mechanism of material degradation and bone formation has not yet been fully clarified (Zerbo *et al.*, 2004). However, ongoing research to find more resorbable CaP materials is required for highly predictable surgical procedures to increase levels of bone formation over a shorter healing period and to maintain the stability of implant insertion and the strength of its anchorage (Xie *et al.*, 2012).

It has been reported that the higher porosity of TCP (65%) resulted in greater bone regeneration and particle degradation in patient biopsies sampled 6 months after SFA (Knabe *et al.*, 2008b; Knabe and Ducheyne, 2008; Stiller *et al.*, 2009). Such studies offer profound insights into the behavior of this synthetic BSM in patients, leading to the search for a new BSM that can be used clinically. A recent study has focused on examining the effect of gender, age, hormone, BMI, and other host factors on bone reconstruction after SFA using β-TCP. The results of this study show that higher degrees of bone formation and osteogenic marker expression were linked to higher levels of E2 and increased BMI, after 6 months of healing (Knabe *et al.*, 2017d). Numerous studies have contributed to broadening our understanding of how bioactive ceramics stimulate bone tissue formation (Ducheyne and Qiu, 1999; Knabe, Adel-Khattab and Ducheyne, 2017). However, clarifying the effect of individual-patient parameters on the osteogenic capability of these BSMs is of crucial importance to select adequate BSM and optimize treatment regimens (Knabe *et al.*, 2017d).

In order to improve osteogenic potency of CaP, the introduction of silicon (Si) to CaPs has been suggested (Patel *et al.*, 2002; Pietak *et al.*, 2007; Bohner, 2009; Fielding, Bandyopadhyay and Bose, 2012). The physiological role of silicon (> 0.5 wt. %) in the early stages of bone mineralization and connective tissue regrowth was initially reported by Carlisle (Carlisle, 1976) and has been recognized as an essential trace component in the bone formation process (Pietak *et al.*, 2007). In Si-substituted CaP ceramics, the addition of silicon can stimulate biological activity by transforming the material surface

to a biologically equivalent HA, increasing the solubility of the material and generating a large electronegative surface (Pietak *et al.*, 2007; Bose *et al.*, 2013). A study by Patel *et al*. showed that the bioactivity of Si-doped HA (0.8 wt.%) in a rabbit model was significantly enhanced by the addition of Si ions into its HA structure compared to phase-pure HA ceramics (Patel *et al.*, 2002). Furthermore, an ovine model study by Wheeler *et al.* compared the efficiency of Si-CaP with autograft on lumbar spinal fusion, noting that Si-HA was biomechanically, radiographically, and histologically relatively equal to autograft forming a solid, intertransverse process fusion. Both grafts had achieved a 100% bone bridging fusion 6 months after healing (Wheeler *et al.*, 2007).

There is conclusive evidence that SiO_2/ZnO doped TCP scaffolds using 3D printing not only promote osteoblastic proliferation and differentiation of bone marrow stromal cells *in vitro* (Fielding, Bandyopadhyay and Bose, 2012), but also improve osteogenesis and neovascularization *in vivo* compared to the pure composition (Fielding, Bandyopadhyay and Bose, 2012; Bose *et al.*, 2013). More recently, the use of Si-CAOP achieved significantly higher rates of bone apposition in humans compared to β-TCP after 6 months of augmentation (Knabe *et al.*, 2017b), and in sheep compared to Si-TCP and native TCP at 2 weeks, 1, 3, 6, 12 and 18 months after implantation (Knabe *et al.*, 2018). However, despite these findings, there have been a few clinical studies comparing the effectiveness of different CaP materials with varying properties on bone formation. However, while the effect of Si-substituted CAOP seems clear, less is known about its detailed bioactivity or how it degrades and is remodeled after 6 months of implantation.

Therefore, this study tested the hypothesis that Si-CAOP (Osseolive™) material may enhance more bone regeneration when compared to pure β-TCP (Cerasorb™ M) as reference material, 6 months after sinus grafting. The study allowed us to provide more comprehensive data about the predictability and success of the Si-CAOP material, compared to the clinically established β-TCP, in implant dentistry. Hard tissue histology, histomorphometry, and immunohistochemistry analysis were used to examine the osteogenic potential and osteogenic marker expression of both test materials to characterize the different stages of bone maturation and formation in cells and tissue components. To successfully display adequate bioactivity and biodegradability, these

materials should be able to differentiate osteogenic cells into osteoblasts on their surfaces, where they lay down the bone matrix and induce the mineralization process (Ducheyne and Qiu, 1999; Stiller *et al.*, 2014). The gene and protein expression involved in osteoblastic differentiation is characterized by three biological stages: cellular proliferation, cellular maturation, and matrix mineralization. An array of osteogenic markers has been established as useful means for studying the influence of BSMs on the different stages of osteoblastic differentiation *in vitro* and *in vivo* (Knabe *et al.*, 2004a, 2008a, 2017d). The expression of these markers was detected in cellular and bone matrix components (Knabe *et al.*, 2018). Type I collagen is expressed during the early stages of osteoblastic proliferation and ECM synthesis, while ALP is expressed during the maturation of ECM and the expression of OC and BSP takes place during the third stage of ECM mineralization (Knabe *et al.*, 2004a; Knabe, Adel-Khattab and Ducheyne, 2017).

The present study examined the effect of Si-CAOP on osteogenesis and osteogenic marker expression in comparison to β-TCP after augmenting the 24 maxillary sinus floors, considering the amount of newly formed bone as well as the residual particles. According to the bone histomorphometric data, new formation of cancellous bone and matrix mineralization was noted in each sinus floor for both patient groups after healing, and there was still active progression of bone formation from the sinus floors in the apical direction. Patient group A showed a higher formation of trabecular bone with a significantly higher degradation of Si-CAOP, when compared to patient group B. This may be related to the higher degree of solubility and degradability of these particles, as illustrated in the previous studies (Berger, Gildenhaar and Ploska, 1995; Knabe, Adel-Khattab and Ducheyne, 2017; Knabe *et al.*, 2017b, 2018).

Besides, ingrowth of bone tissue in pores of the degrading material in combination with good bony integration of these particles was also clearly identified in biopsies sampled after Si-CAOP and β-TCP implantation. These results demonstrated Increased amounts of newly formed bone noted apically, i.e. close to the Schneiderian membrane in association with a significantly higher particle degradation of the highly porous Si-CAOP particles centrally and apically (p<0.05), compared to TCP. Similar findings were

reported by Knabe *et al.* (Knabe *et al.*, 2017b), resulting in the Si-CAOP particles being more highly degraded than the polygonal β-TCP particles, leading in turn to greater amount of bone regeneration in the sinus floors. There was a higher tendency for particulate Si-CAOP to disintegrate and actively remodel into the newly formed osseous trabeculae with good bone-bonding behavior when compared to the TCP group. In this context, it may also be useful to acquire histomorphometric data on the bone-particle contact of the TCP group in future studies.

The human clinical study furthermore revealed that the Si-CAOP biopsies have the potential to enhance blood vessel formation when stained immunohistochemically with vWF. It was only four sections stained for this marker. Thus, performing analysis of these markers on hard tissue sections of a higher number of biopsies would allow for the characterization of the newly formed blood vessels and permit more accurate statistical analysis to be carried out. To this end, a new methodology is currently under development, which facilitates preparing a higher number of resin-embedded sections from biopsies, which are only 2.2 mm in diameter.

The immunohistochemical evaluation was also performed centrally and apically to characterize the protein expression of an array of osteogenic parameters 6 months after augmentation. More intense immunostaining for OC, Col I, BSP and ALP in the osteoid component of the central and apical areas, and for OC and BSP in the mineralized bone matrices in the central area were noted for the Si-CAOP group A. The expression of OC and BSP in the newly formed osteoid and mineralized bone matrices is indicative of good bone regeneration. In the silicon doped CAOP group, bone formation and matrix mineralization had developed to a greater extent after 6 months of SFA than in the control group. However, this was still ongoing, as mild to moderate OC, Col I and BSP expression was observed in the unmineralized fibrous matrices of the osteogenic-cell rich mesenchyme. The β-TCP sites displayed a greater level of OC, Col I and BSP staining in the unmineralized fibrous matrices showing that bone matrix formation and mineralization were advancing more slowly than in the Si-CAOP sites, although there was still active progression at this point. Moreover, a positive ALP expression in the cells and matrix components surrounding the residual degrading materials were shown in

both patient groups. Still, relatively large differences were detected between the Si-CAOP and β-TCP groups.

Based on these findings, the variation in material properties including Si-release and calcium uptake at the biomaterial surface of Si-CAOP and β-TCP (Knabe *et al.*, 2017b, 2018) appears to influence bone regeneration and particle degradation, as well as the expression levels of various osteogenic markers in the cell and tissue components of the newly formed bone. The slight difference in porosity may also have contributed to the greater levels of bone formation and particle degradation observed in the apical areas of the Si-CAOP biopsies.

In our study, the assessment of the amount of bone formed was relied on two-dimensional histological data generated from one section of each biopsy, and no postoperative radiological analysis such as CBCT or synchrotron microtomography (SCT) was performed. It would be therefore preferable to compliment histological data with CBCT or SCT data to demonstrate volume stability of the grafted area in order to confirm the consistency of our results. In this context, a study by Stiller *et al.* concluded that SCT was a reliable and non-invasive assessment tool to examine the three-dimensional microarchitecture of biopsies in terms of visualization of bone formation morphology and organization of bone trabeculae (Stiller *et al.*, 2009). In addition, CBCT assessment has been shown to be a valuable tool for determining volumetric changes in graft volume at four times: pre-operatively, immediately postoperatively, 6 months after SFA, and 2.5 years after SFA (Okada *et al.*, 2016).

After 6 months of healing, our current study found that the crystalline-particulate Si-CAOP and spherical-particulate β-TCP had degraded, integrated, remodeled, and were to a considerable degree replaced by bone tissue, although there was no clear evidence about how the particle resorption occurred or how it affected the biological tissue response. In order to determine whether particle resorption occurred by chemical dissolution or osteoclastic activity, Si-CAOP biopsies were stained for TRAP-positive osteoclasts. TRAP staining, however, revealed no positive staining for osteoclasts. Our findings are consistent with previous results showing that the degradation of Si-CAOP

containing the main crystalline phase $Ca_2KNa(PO_4)_2$ and β-TCP seems more likely to be due to physicochemical dissolution rather than osteoclastic activity after SFA in humans (Müller-Mai *et al.*, 1997; Knabe *et al.*, 2008b; Knabe, Adel-Khattab and Ducheyne, 2017). In contrast, for HA-based materials, It was reported that they were resorbed mainly through osteoclastic activity (Schepers *et al.*, 1991), whereas the chemical dissolution appeared to be the main cause of the TCP (Zerbo *et al.*, 2005) and BG 45S5 (Tadjoedin *et al.*, 2002) degradation, and osteoclasts play only a minor role in TCP substitution by bone.

Such differences in degradation behavior between HA, TCP and BG45S5 are linked to higher pH levels during the particle dissolution process (Peters and Reif, 2004). The differences observed between the two used materials may be correlated to surface topography and chemistry as well as the presence of silicon, which could have a profound effect on the resorption mechanism. In this context, the results show that both Si-CAOP and native TCP support osteoblast differentiation and bone matrix formation and maturation, however, enhanced more strongly by Si-CAOP. This may be linked to physicochemical properties of silica, which have been shown to enhance the effect of CaP ceramics on osteoblast function, and bone matrix formation. This comparative study demonstrated that using Si-CAOP for SFA can support implant placement and provide better results than using TCP particles.

Another eight biopsies sampled with Si-CAOP particles showed increased degrees of bone regeneration and high degradation rates during histological analysis. Nevertheless, they were excluded from this study as the patients suffered from systemic diseases such as hypertension, diabetes, and blood disorders. For some samples, the histomorphometric analysis was performed.

Our study examined the biological effect of the Si-CAOP particles on bone and blood vessel formation after SFA and characterized their biodegradation in order to evaluate whether their higher solubility was beneficial. A vital aspect of these particles is the optimization of their chemical and structural properties for increasing the bone formation rate. The biological performance can be altered by doping CAOP with silica,

which improves their bioactive properties. The introduction of silica to these particles yield improved bone formation rates as well as enhanced osteogenic marker expressions *in vivo* (Knabe *et al.*, 2017b). The comparison of the two treatment groups confirmed the resorbability of both porous materials and their considerable substitution by the newly formed bone in the augmented sinus floors, with no complications such as adverse tissue reactions or implant failure reported in patients. Our histological evaluation showed that both materials clearly facilitated bone regeneration of resorbed alveolar ridges in the human posterior maxilla and greater primary stability during implant placement in patients augmented with Si-CAOP, with higher biodegradability and greater amounts of bone formation compared to β-TCP.

Although our study showed differences in the quantity of bone formed depending on the use of two different materials, these differences were not statistically significant. In Si-CAOP sites, the particles are rapidly replaced after 6 months of healing, whereas in β-TCP sites, the particles are more likely to be replaced continuously with longer healing times, and remodeling of woven bone into the trabeculae of the highly cancellous original microanatomy of the maxillary bone had not reached as an advanced stage as Si-CAOP sites . Bone formation and matrix mineralization were still in progress around the highly degraded Si-CAOP particles, whereas in the β-TCP group matrix mineralization of the unmineralized fibrous matrix of the osteogenic mesenchyme had not reached as an advanced stage as observed with Si-CAOP group. This may be attributed to high bone-particle contact and the migration of osteoblasts into the micro-pores of the Si-CAOP particles.

The Si-CAOP group exhibited superior bioactive and osteogenic properties to the control group, and thereby confirmed the tested hypothesis. It also is important that significant differences with regard to the amount of formed bone and expressions of osteogenic markers were observed histologically between the two types of grafting materials. However, these findings confirm the need for evaluating further properties of the Si-CAOP material by analysis of the radiological data with respect to volume stability of the grafted area and examining of angiogenic markers in resin-embedded sections, in order to characterize the angiogenic properties.

In conclusion, both studied grafting materials enabled bony regeneration of resorbed alveolar ridges by SFA in the human posterior maxilla, with Si-CAOP displaying higher biodegradability and inducing greater bone formation when compared to β-TCP. An important finding was that the first immunohistochemical results showed that Si-CAOP enhanced neovascularization during new bone formation. This study demonstrates the higher stimulatory effect of Si-CAOP (75% porosity) on osteogenesis and osteogenic marker expressions, thereby confirming its superiority to β-TCP. Consequently, these findings generated reliable histological, immunohistochemical, and histomorphometric data for the evidence-based application of this promising bioactive material.

Based on the findings of our study, it can be concluded that Si-CAOP has great potential use for SFA in humans. However, there is still further work to be performed to optimize the characterization of the osteogenic capacity of these particles. A next prospective study involving a larger patient number, a split-mouth design, determining the bone-particle contact, analysis of cone beam-CT-data for assessing the volume stability of the augmented area and investigation of angiogenesis, is warranted to further confirm the high osteogenic and angiogenic capacity of the Si-CAOP materials for orofacial bone regeneration. Thus, this comprehensive database can then be integrated with the morphological measurement outcomes providing detailed information and validating the therapeutic efficacy of the uses of silicon-containing calcium alkali orthophosphate Osseolive in a clinical setting.

5. Summary

Over the last 25 years, the use of dental implants to replace missing teeth has become a standard treatment in modern dentistry. However, implant therapy can be a challenge in patients with insufficient bone volume. Pre-implantology procedures for alveolar ridge augmentation serve as the basis for creating sufficient bone volume and quality for oral rehabilitation in these patients. Sinus floor augmentation is a well-recognized procedure for the augmentation of the atrophic alveolar ridges of the posterior maxilla. Although autologous bone grafts are the gold standard, they have the disadvantages of the additional surgical operations required, the risk of morbidity in the donor region, and the need for general anesthesia to obtain iliac crest grafts, which have led to an increasing search for alternatives. This has led to intensive research to develop suitable synthetic bone replacement materials. Ideal bone graft substitutes should serve as a guide and provide a surface in which bone formation is induced. The migration of osteoprogenitor cells to the material surface, which differentiate into osteoblasts and secrete bone matrix, results in mineralized bone matrix. In addition, the bone graft should be relatively rapidly resorbable in order to resorb within the newly formed bone in case of rapid bone formation. This should lead to complete replacement by the new, functional bone tissue. This is of great importance for ridge augmentation in view of inserting dental implants into the augmented areas, since osseointegration can only occur between the implant surface and the bone tissue. The use of β-tricalcium phosphates (β-TCP), which are osteoconductive, as bone substitute material for ridge augmentation has become an established procedure. However, the resorption rate of β-TCP is 1-2 years in humans. A new type of calcium phosphate ceramics are glassy crystalline silica-containing calcium alkali orthophosphates with the main crystalline phase $Ca_2KNa(PO_4)_2$, which have been developed to achieve a higher chemical solubility and degradability. Previous *in vitro* and *in vivo* studies have shown that these materials had a stronger stimulating effect on osteoblastic function, bone formation and osteogenesis than tricalcium phosphates. In the present clinical study, the effect of silica- containing calcium alkali orthophosphate (Si-CAOP, Osseolive™) on osteogenesis and osteogenic marker expression was studied in comparison to β-tricalcium phosphates (β-TCP, Cerasorb™ M) in biopsies obtained 6 months after sinus floor

augmentation in 24 patients. Cylindrical biopsies were processed for immunohistochemical investigations on hard tissue sections using the osteogenic markers osteocalcin, collagen type I, bone sialoprotein, and alkaline phosphatase. Immunohistochemical detection of the angiogenic marker (von Willebrand factor) was also established on some Osseolive™ samples for the investigation of blood vessel formation. Histomorphometric analysis of the histological sections was performed in two areas of interest: central and apical near the Schneiderian membrane. The area fraction of the bone and particles was measured histomorphometrically in both areas. Furthermore, a semi-quantitative analysis of osteogenic marker expression in osteoblasts, osteocytes, mesenchymal cells, fibrous matrix, osteoid and bone matrix was performed. In addition, a tartrate-resistant acid phosphatase stain was used to detect osteoclast activity. Our histological evaluation showed that both materials caused bone matrix deposition within the particles, bone ingrowth and increasing bone formation, which was still actively progressing in an apical direction 6 months after implantation. This was accompanied by an increasing resorption of the bone substitute material. This process was more advanced in biopsies grafted with the Si-CAOP 6 months after sinus floor augmentation than in biopsies grafted with β-TCP. No complications, such as undesirable inflammatory tissue reactions or implant loss, were observed in either patient group. In the central region of the specimens, bone formation and resorption varied between the two materials, but these differences were not statistically significant, while in the apical region of the Si-CAOP augmented biopsies there was higher bone formation and significantly ($p \leq 0.05$) greater particle resorption than in biopsies after augmentation with β-TCP. In the Si-CAOP group, this was associated with higher expression of osteogenic markers in the osteoid, osteocytes and bone matrix. In initial studies on angiogenic marker expression, the Si-CAOP particles showed a promotion of vascular ingrowth during bone formation. In summary, both test materials enabled bony regeneration of resorbed alveolar ridges by sinus floor augmentation in the human posterior maxilla, with Si-CAOP displaying higher biodegradability and inducing stronger bone formation when compared to the β-TCP material. This work confirmed the higher stimulatory effect of Si-CAOP with a porosity of 75% on osteogenesis in 12 patients by generating comprehensive histological,

immunohistochemical and histomorphometric data for an evidence-based application of this promising bioactive material. A further study will include a larger number of patients, a split-mouth design, the determination of the bone-particle contact, further investigations on angiogenesis and investigations on the volume stability of the augmentation material through the evaluation of cone-beam CT data in order to expand the database for the evidence-based application of the silicon-containing calcium-alkali orthophosphate Osseolive.

6. German summary

Wirkung eines hoch bioaktiven Knochenersatzmaterials auf Calcium-Alkali-Orthophosphat-Basis im Vergleich zu Tricalciumphosphat auf die Osteogenese nach Sinusbodenaugmentation bei Patienten

In den letzten 25 Jahren hat sich die Verwendung von Zahnimplantaten zum Ersatz fehlender Zähne zu einer Standardbehandlung in der modernen Zahnmedizin entwickelt. Die Implantattherapie kann jedoch bei Patienten mit unzureichendem Knochenvolumen eine Herausforderung darstellen. Präimplantologisches Verfahren zur Alveolarkammaugmentation dienen bei diesen Patienten als Grundlage für die Schaffung einer ausreichenden Knochenmenge und -qualität für die orale Rehabilitation. Die Sinusboden-Augmentation ist ein anerkanntes Verfahren zur Augmentation atrophischer Kieferkämme des hinteren Oberkiefers. Obwohl autologe Knochentransplantate den Goldstandard darstellen, sind diese mit den Nachteilen des zusätzlich erforderlichen chirurgischen Zweiteingriffes, dem Risiko der Morbidität in der Spenderregion und der Notwendigkeit einer Vollnarkose zur Gewinnung von Beckenkammtransplantaten behaftet, welches eine zunehmende Suche nach Alternativen bedingt hat. Dies hat zu intensiver Forschung zur Entwicklung geeigneter synthetischer Knochenersatzmaterialien geführt. Ideale Knochenersatzmaterialien sollten als Leitschiene dienen, an deren Oberfläche die Knochenbildung induziert wird. Durch Migration von Osteoprogenitorzellen zur Materialoberfläche, die zu Osteoblasten differenzieren und Knochenmatrix sezernieren, entsteht dabei mineralisierte Knochenmatrix. Darüber hinaus sollte das Knochentransplantat relativ schnell resorbierbar sein, um bei rascher Knochenbildung im neugebildeten Knochen zu resorbieren. Dies sollte zu einem vollständigen Ersatz durch das neue, funktionsfähige Knochengewebe führen. Dies ist bei der Kieferkammaugmentation für die Insertion des Implantats in die augmentierten Areale von großer Bedeutung, da eine Osseointegration nur zwischen Implantatoberfläche und Knochengewebe erfolgen kann. Die Verwendung von β-Tricalciumphosphaten (β-TCP), welche osteokonduktiv sind, als Knochenersatzmaterial für die Kieferkammaugmentation ist ein etabliertes Verfahren geworden. Die Resorptionsrate von β-TCP liegt zwischen 1-2 Jahren beim Menschen. Ein neuer Typ von Calciumphosphat-Keramik sind glasig-kristalline Siliziumdioxid

enthaltene Calcium-Alkali-Orthophosphate mit der kristallinen Hauptphase $Ca_2KNa(PO_4)_2$, welche entwickelt wurden, um eine höhere chemische Löslichkeit und Abbaubarkeit zu erreichen. Vorausgegangene *in vitro*- und *in vivo*-Studien haben gezeigt, dass diese Materialien eine stärker stimulierende Wirkung auf die osteoblastische Zellfunktion, die Knochenbildung und die Osteogenese ausübten als Tricalciumphosphate. In der vorliegenden klinischen Studie wurde die Wirkung des Siliciumdioxid-haltigen Calcium-Alkali-Orthophosphates (Si-CAOP, Osseolive™) auf die Osteogenese und die osteogene Markerexpression im Vergleich zu βTricalciumphosphat (β-TCP, Cerasorb™ M) in Bioptaten, die 6 Monaten nach Sinusbodenaugmentation gewonnen wurden, bei 24 Patienten untersucht. Zylindrisch Biopsien wurden für immunhistochemische Untersuchungen an Hartgewebsschnitten unter Verwendung der osteogenen Marker Osteocalcin, Kollagen Typ I, Bonesialoprotein und alkalische Phosphatase aufbereitet. An einigen Osseolive™ Proben wurden auch der immunhistochemische Nachweis des angiogenen Markers (von Willebrand-Faktor) zur Untersuchung der Blutgefäßbildung etabliert. Die histomorphometrische Analyse der histologischen Schnitte wurde in zwei Bereichen von Interesse durchgeführt: zentral und apikal nahe der Schneider'schen Membran. Die Flächenanteile des Knochens und der Partikel wurde in beiden Bereichen histomorphometrisch gemessen. Weiterhin wurde eine semiquantitative Auswertung der osteogenen Markerexpression in Osteoblasten, Osteozyten, mesenchymalen Zellen, fibröser Matrix, Osteoid und Knochenmatrix durchgeführt. Darüber hinaus wurde eine Tartrat-resistente saure Phosphatasefärbung zum Nachweis der Osteoklastenaktivität verwendet. Unsere histologischen Auswertungen zeigten, dass beide Materialien eine Knochenmatrixablagerung innerhalb der Partikel, Knocheneinwachsen und eine zunehmende Knochenbildung, die 6 Monaten nach Implantation noch aktiv in apikale Richtung voranschreitete, bewirkten. Dies war von einer zunehmenden Resorption des Knochenersatzmaterials begleitet. Dieser Prozess war bei Osseolive 6 Monate nach Sinusbodenaugmantation weiter vorangeschritten als bei β-TCP. Bei beiden Materialien waren dabei bei keinen Patienten irgendwelche Komplikationen wie unerwünschte entzündliche Gewebereaktionen oder Implantatverlust zu verzeichnen. Im zentralen Bereich der Proben variierten Knochenbildung und -abbau zwischen den beiden Materialien, diese Unterschiede

waren jedoch nicht statistisch signifikant, während im apikalen Bereich der mit Si-CAOP augmentierten Bioptate eine höhere Knochenbildung und ein signifikant ($p \leq 0.05$) größerer Partikelabbau vorlag als in Bioptaten nach Augmentation mit β-TCP. Bei Si-CAOP war dies mit einer höheren Expression osteogener Marker im Osteoid, den Osteocyten und der Knochenmatrix assoziiert. Die Si-CAOP Partikel zeigten in ersten Untersuchungen zur angiogenen Markerexpression eine Förderung des Einwachsens von Gefäßen während der Knochenbildung. Zusammenfassend lässt sich feststellen, dass beide Testmaterialien eine knöcherne Regeneration resorbierter Alveolarkämme mittels Sinusbodenaugementation im menschlichen hinteren Oberkiefer ermöglichten, wobei sich für Si-CAOP im Vergleich zum β-TCP-Material eine höhere biologische Abbaubarkeit und eine stärkere Knochenbildung zeigte. Diese Arbeit bestätigte die höhere stimulierende Wirkung von Si-CAOP mit einer Porosität von 75 % auf die Osteogenese bei 12 Patienten, indem umfassende histologische, immunhistochemische und histomorphometrische Daten für eine evidenzbasierte Anwendung dieses vielversprechenden bioaktiven Materials generiert werden konnten.

Eine weiterführende Studie wird eine größere Patientenzahl, ein Split-Mouth-Design, die Bestimmung des Knochen-Partikel-Kontakt, weiterführende Untersuchungen zur Angiogenese sowie Untersuchungen zur Volumenstabilität des Augmentats durch die Auswertung von Cone-Beam-CT-Daten einschließen, um die Datenbasis zur evidenzbasierten Anwendung des siliziumhaltigen Calcium-Alkali-Orthophosphates Osseolive zu erweitern.

7. References

Aghaloo, T. L. and Moy, P. K. (2007) 'Which hard tissue augmentation techniques are the most successful in furnishing bony support for implant placement?', *The International journal of oral & maxillofacial implants*, 22 Suppl, pp. 49–70. Available at: http://www.ncbi.nlm.nih.gov/pubmed/18437791.

Berger, G., Gildenhaar, R. and Ploska, U. (1995) 'Rapid resorbable, glassy crystalline materials on the basis of calcium alkali orthophosphates', *Biomaterials*, 16(16), pp. 1241–1248. doi: 10.1016/0142-9612(95)98131-W.

Berger, G., Mücke, U. and Harbich, K. W. (2003) 'Determination of the internal surface of spongiosa-like ceramic scaffolds using light microscopy and x-ray refraction technique', in *Key Engineering Materials*, 240-242, pp. 469–472. doi: 10.4028/www.scientific.net/kem.240-242.469.

Van Den Bergh, J. P. A., Ten Bruggenkate, C. M., Disch, F. J. M. and Tuinzing, D. B. (2000) 'Anatomical aspects of sinus floor elevations', *Clinical Oral Implants Research*, 11(3), pp. 256-265. doi: 10.1034/j.1600-0501.2000.011003256.x.

Bohner, M. (2009) 'Silicon-substituted calcium phosphates - A critical view', *Biomaterials*. Elsevier Ltd, 30(32), pp. 6403-6406.
doi: 10.1016/j.biomaterials.2009.08.007.

Bose, S., Fielding, G., Tarafder, S. and Bandyopadhyay, A. (2013) 'Understanding of dopant- induced osteogenesis and angiogenesis in calcium phosphate ceramics', *Trends in Biotechnology*, 31(10), pp. 594-605. doi: 10.1016/j.tibtech.2013.06.005.

Boyne, P. J. and James, R. A. (1980) 'Grafting of the maxillary sinus floor with autogenous marrow and bone', *Journal of Oral Surgery*, 38(8), 613–616.

Bunte, M. and Strunz, V. (1977) 'Ceramic augmentation of the lower jaw', *Journal of Maxillofacial Surgery*, 5(C), pp. 303–309. doi: 10.1016/S0301-0503(77)80123-9.

Buser, D., Dula, K., Hirt, H. P. and Schenk, R. K. (1996) 'Lateral ridge augmentation using autografts and barrier membranes: A clinical study with 40 partially edentulous patients', *Journal of Oral and Maxillofacial Surgery*, *54*(4), pp. 420-432. doi: 10.1016/S02782391(96)90113-5.

Buser, D., Dula, K., Hess, D., Hirt, H. P. and Belser, U. C. (1999) 'Localized ridge augmentation with autografts and barrier membranes', *Periodontology 2000*, 19(1), pp. 151–163. doi: 10.1111/j.1600-0757.1999.tb00153.x.

Carlisle, E. M. (1976) 'In vivo Requirement for Silicon in Articular Cartilage and Connective Tissue Formation in the Chick', *The Journal of Nutrition*. Oxford University Press (OUP), 106(4), pp. 478–484. doi: 10.1093/jn/106.4.478.

Clark, D. and Levin, L. (2016) 'Dental implant management and maintenance: How to improve long-term implant success?', *Quintessence International*, 47(5), pp. 417–423. doi: 10.3290/j.qi.a35870.

Cordaro, L., Bosshardt, D. D., Palattella, P., Rao, W., Serino, G. and Chiapasco, M. (2008) 'Maxillary sinus grafting with Bio-Oss® or Straumann® Bone Ceramic: Histomorphometric results from a randomized controlled multicenter clinical trial', *Clinical Oral Implants Research*, 19(8), pp. 796–803. doi: 10.1111/j.1600-0501.2008.01565.x.

Dorozhkin, S. V. and Epple, M. (2002) 'Biological and medical significance of calcium phosphates', *Angewandte Chemie - International Edition*, *41*(17), pp. 3130-3146.doi: 10.1002/1521-3773(20020902)41:17<3130::AID-ANIE3130>3.0.CO;2-1.

Drage, N. A., Palmer, R. M., Blake, G., Wilson, R., Crane, F. and Fogelman, I. (2007) 'A comparison of bone mineral density in the spine, hip and jaws of edentulous subjects',

Clinical Oral Implants Research, 18(4), pp. 496–500. doi: 10.1111/j.1600-0501.2007.01379.x.

Ducheyne, P. and Qiu, Q. (1999) 'Bioactive ceramics: The effect of surface reactivity on bone formation and bone cell function', *Biomaterials*, 20(23–24), pp. 2287–2303. doi: 10.1016/S0142-9612(99)00181-7.

Esposito, M., Grusovin, M. G., Kwan, S., Worthington, H. V. and Coulthard, P. (2009) 'Interventions for replacing missing teeth: Bone augmentation techniques for dental implant treatment', *Australian Dental Journal*, *54*(1), pp. 70-71. doi: 10.1111/j.18347819.2008.01093.x.

Esposito, M., Grusovin, M. G., Rees, J., Karasoulos, D., Felice, P., Alissa, R., Worthington. H. and Coulthard, P. (2010) 'Effectiveness of sinus lift procedures for dental implant rehabilitation: a Cochrane systematic review.', *European journal of oral implantology*, 3(1), pp. 7–26. Available at: http://www.ncbi.nlm.nih.gov/pubmed/20467595.

Fernyhough, J. C., Schimandle, J. J., Weigel, M. C., Edwards, C. C. and Levine, A. M. (1992) 'Chronic donor site pain complicating bone graft harvesting from the posterior iliac crest for spinal fusion', *Spine*, 17(12), pp. 1474 —1480. doi: 10.1097/00007632-199212000-00006.

Fielding, G. A., Bandyopadhyay, A. and Bose, S. (2012) 'Effects of silica and zinc oxide doping on mechanical and biological properties of 3D printed tricalcium phosphate tissue engineering scaffolds', *Dental Materials*. The Academy of Dental Materials, 28(2), pp. 113–122. doi: 10.1016/j.dental.2011.09.010.

Funato, A., Yamada, M. and Ogawa, T. (2013) 'Success Rate, Healing Time, and Implant Stability of Photofunctionalized Dental Implants', *The International Journal of Oral & Maxillofacial Implants*, 28(5), pp. 1261–1271. doi: 10.11607/jomi.3263.

Gapski, R., Wang, H. L., Mascarenhas, P. and Lang, N. P. (2003) 'Critical review of immediate implant loading', *Clinical Oral Implants Research*, 14(5), pp. 515–527. doi: 10.1034/j.16000501.2003.00950.x.

Gaviria, L., Pearson, J. J., Montelongo, S. A., Guda, T. and Ong, J. L. (2017) 'Three-dimensional printing for craniomaxillofacial regeneration', *Journal of the Korean Association of Oral and Maxillofacial Surgeons*, 43(5), pp. 288. doi: 10.5125/jkaoms.2017.43.5.288.

Göçmen, G. and Özkan, Y. (2017) 'Maxillary Sinus Augmentation for Dental Implants', in *Paranasal Sinuses*, 39. doi: 10.5772/intechopen.69063.

Goldberg, A. F. and Barka, T. (1962) 'Acid Phosphatase Activity in Human Blood Cells', *Nature*, 195(4838), pp. 297. doi: 10.1038/195297a0.

Guarino, V., Causa, F. and Ambrosio, L. (2007) 'Bioactive scaffolds for bone and ligament tissue', *Expert Review of Medical Devices*, 4(3), pp. 405–418. doi: 10.1586/17434440.4.3.405.

Hench, L. L., Splinter, R. J., Allen, W. C. and Greenlee, T. K. (1971) 'Bonding mechanisms at the interface of ceramic prosthetic materials', *Journal of Biomedical Materials Research*, *5*(6), pp. 117-141. doi: 10.1002/jbm.820050611.

Hench, L. L. (2015) 'The future of bioactive ceramics', *Journal of Materials Science: Materials in Medicine*. Kluwer Academic Publishers, 26(2), pp. 86. doi: 10.1007/s10856-015-5425-3.

Jaffin, R. A. and Berman, C. L. (1991) 'The Excessive Loss of Branemark Fixtures in Type IV Bone: A 5-Year Analysis', *Journal of Periodontology*, *62*(1), pp. 2-4. doi: 10.1902/jop.1991.62.1.2.

Jensen, S. S., Yeo, A., Dard, M., Hunziker, E., Schenk, R. and Buser, D. (2007) 'Evaluation of a novel biphasic calcium phosphate in standardized bone defects. A histologic and histomorphometric study in the mandibles of minipigs', *Clinical Oral Implants Research*, 18(6), pp. 752–760. doi: 10.1111/j.1600-0501.2007.01417.x.

Kaptein, M. L. A., Hoogstraten, J., De Putter, C., De Lange, G. L. and Blijdorp, P. A. (1998) 'Dental implants in the atrophic maxilla: Measurements of patients' satisfaction and treatment experience', *Clinical Oral Implants Research*, *9*(5), pp. 321-326. doi: 10.1034/j.16000501.1998.090505.x.

Katranji, A., Fotek, P. and Wang, H. L. (2008) 'Sinus augmentation complications: Etiology and treatment', *Implant Dentistry*, *17*(3), pp. 339-349. doi: 10.1097/ID.0b013e3181815660.

Kim, Y., Nowzari, H. and Rich, S. K. (2013) 'Risk of Prion Disease Transmission through Bovine-Derived Bone Substitutes: A Systematic Review', *Clinical Implant Dentistry and Related Research*, 15(5), pp. 645–653. doi: 10.1111/j.1708-8208.2011.00407.x.

Knabe, C., Berger, G., Gildenhaar, R., Klar, F. and Zreiqat, H. (2004a) 'The modulation of osteogenesis in vitro by calcium titanium phosphate coatings', *Biomaterials*, 25(20), pp. 4911– 4919. doi: 10.1016/j.biomaterials.2004.01.059.

Knabe, C., Berger, G., Gildenhaar, R., Meyer, J., Howlett, C. R., Markovic, B. and Zreiqat, H. (2004b) 'Effect of rapidly resorbable calcium phosphates and a calcium phosphate bone cement on the expression of bone related genes and proteins in vitro', *Journal of Biomedical Materials Research - Part A*, 69(1), pp. 145–154. doi: 10.1002/jbm.a.20131.

Knabe, C., Kraska, B., Koch, C., Gross, U., Zreiqat, H. and Stiller, M. (2006) 'A method for immunohistochemical detection of osteogenic markers in undecalcified bone sections', *Biotechnic and Histochemistry*, 81(1), pp. 31–39. doi: 10.1080/10520290600725474.

Knabe, C., Houshmand, A., Berger, G., Ducheyne, P., Gildenhaar, R., Kranz, I. and Stiller, M. (2008a) 'Effect of rapidly resorbable bone substitute materials on the temporal expression of the osteoblastic phenotype in vitro', *Journal of Biomedical Materials Research - Part A*, *84*(4), pp. 856-868. doi: 10.1002/jbm.a.31383.

Knabe, C., Koch, C., Rack, A. and Stiller, M. (2008b) 'Effect of β-tricalcium phosphate particles with varying porosity on osteogenesis after sinus floor augmentation in humans', *Biomaterials*, *29*(14), pp. 2249-2258. doi: 10.1016/j.biomaterials.2008.01.026.

Knabe, C., Berger, G., Gildenhaar, R., Ducheyne, P. and Stiller, M. (2010) 'Novel, Rapidly Resorbable Bioceramic Bone Grafts Produce a Major Osteogenic Effect - The Pre-Clinical Evidence', *Advances in Science and Technology*, 76, pp. 214-223. doi: 10.4028/www.scientific.net/ast.76.214.

Knabe, C., Lopez Heredia, M., Barnemitz, D., Genzel, A., Peters, F. and Hübner, W. D. (2014) 'Effect of Silicon-Doped Calcium Phosphate Bone Substitutes on Bone Formation and Osteoblastic Phenotype Expression *In Vivo*', *Key Engineering Materials*, 614, pp. 31–34. doi: 10.4028/www.scientific.net/kem.614.31.

Knabe, C., Ducheyne, P., Adel-Khattab, D. and Stiller, M. (2017a) 'Chapter 10175 - 7.20 Dental Graft Materials', *Comprehensive Biomaterials II*, pp. 378–405. doi: 10.1016/B978-0-12-803581 8.10175-4.

Knabe, C., Knauf, T., Adel-Khattab, D., Peleska, B., Hübner, W.-D., Peters, F., Rack, A., Gildenhaar, R., Berger, G., Günster, J., Houshmand, A. and Stiller, M. (2017b) 'Effect of a Rapidly Resorbable Calcium Alkali Phosphate Bone Grafting Material on Osteogenesis after Sinus Floor Augmentation in Humans', *Key Engineering Materials*. Trans Tech Publications Ltd, 758, pp. 239–244. doi: 10.4028/www.scientific.net/KEM.758.239.

Knabe, C., Adel-Khattab, D., Kluk, E., Struck, R. and Stiller, M. (2017c) 'Effect of a Particulate and a Putty-Like Tricalcium Phosphate-Based Bone Grafting Material on Bone Formation, Volume Stability and Osteogenic Marker Expression after Bilateral Sinus Floor Augmentation in Humans', *Journal of functional biomaterials*, *8*(3), p. 31. Preprints.org. Retrieved from https://doi:10.20944/PREPRINTS201706.0106.V1.

Knabe, C., Mele, A., Kann, P. H., Peleska, B., Adel-Khattab, D., Renz, H., Reuss, A., Bohner, M. and Stiller, M. (2017d) 'Effect of sex-hormone levels, sex, body mass index and other host factors on human craniofacial bone regeneration with bioactive tricalcium phosphate grafts', *Biomaterials*, *123*, pp. 48-62. doi: 10.1016/j.biomaterials.2017.01.035.

Knabe, C., Adel-Khattab, D., Hübner, W. D., Peters, F., Knauf, T., Peleska, B., Barnewitz, D., Genzel, A., Kusserow, R., Sterzik, F., Stiller, M. and Müller-Mai, C. (2018) 'Effect of silicon-doped calcium phosphate bone grafting materials on bone regeneration and osteogenic marker expression after implantation in the ovine scapula', *Journal of Biomedical Materials Research - Part B Applied Biomaterials*, 107(3), pp. 594-614. doi: 10.1002/jbm.b.34153.

Knabe, C., Adel-Khattab, D. and Ducheyne, P. (2017) '1.12 Bioactivity: Mechanisms ☆', *Comprehensive Biomaterials II*, 1, pp. 291–310. doi: 10.1016/B978-0-12-803581-8.09400-5.

Knabe, C. and Ducheyne, P. (2008) 'Cellular response to bioactive ceramics', in *Bioceramics and their Clinical Applications*, pp. 133–164. doi: 10.1533/9781845694227.1.133.

Knabe, C., Ducheyne, P. and Stiller, M. (2011) 'Dental Graft Materials', *Comprehensive Biomaterials*, 7, pp. 305–324. doi: 10.1016/B978-0-08-055294-1.00224-5.

Legeros, R. Z., Lin, S., Rohanizadeh, R., Mijares, D. and Legeros, J. P. (2003) 'Biphasic calcium phosphate bioceramics: Preparation, properties and applications', *Journal of Materials Science: Materials in Medicine*, 14(3), pp. 201–209. doi: 10.1023/A:1022872421333.

Liu, G., Zhao, L., Zhang, W., Cui, L., Liu, W. and Cao, Y. (2008) 'Repair of goat tibial defects with bone marrow stromal cells and β-tricalcium phosphate', *Journal of Materials Science: Materials in Medicine*, *19*(6), pp. 2367-2376. doi: 10.1007/s10856-007-3348-3.

Liu, X., Chu, P. K. and Ding, C. (2004) 'Surface modification of titanium, titanium alloys, and related materials for biomedical applications', *Materials Science and Engineering R: Reports*, 47(3–4), pp. 49–121. doi: 10.1016/j.mser.2004.11.001.

Lopez-Heredia, M. A., Barnewitz, D., Genzel, A., Stiller, M., Peters, F., Hübner, W. D., Stang, B., Kuhr, A. and Knabe, C. (2014) '*In Vivo* Osteogenesis Assessment of a Tricalcium Phosphate Paste and a Tricalcium Phosphate Foam Bone Grafting Materials', *Key Engineering Materials*, 631, pp. 426-429. doi: 10.4028/www.scientific.net/kem.631.426.

Mastrangelo, F., Nargi, E., Carone, L., Dolci, M., Caciagli, F., Ciccarelli, R., Lutiis, M.A.D., Karapanou, V., Shaik, B. Y., Conti, P. and Teté, S. (2008) 'Tridimensional response of human dental follicular stem cells onto a synthetic hydroxyapatite scaffold', *Journal of Health Science*, 54(2), pp. 154-161. doi: 10.1248/jhs.54.154.

Merten, H. A., Wiltfang, J., Grohmann, U. and Hoenig, J. F. (2001) 'Intraindividual comparative animal study of α- and β-tricalcium phosphate degradation in conjunction with simultaneous insertion of dental implants', *Journal of Craniofacial Surgery*, 12(1), pp. 59–68. doi: 10.1097/00001665-200101000-00010.

Misch, C. E. and Dietsh, F. (1993) 'Bone-grafting materials in implant dentistry', *Implant dentistry*, 2(3), pp. 158 —167. doi: 10.1097/00008505-199309000-00003.

Moore, W. R., Graves, S. E. and Bain, G. I. (2001) 'Review Article Synthetic Bone Graft

Substitutes', ANZ J. Surg., 71(6), pp. 354–361. doi.org/10.1046/j.1440-1622.2001.02128.x.

Müller-Mai, C., Berger, G., Voigt, C., Bakki, B. and Gross, U. (1997) 'The bony reaction to rapidly degradable glass-ceramics based on the new phase Ca2KNa(PO4)2', in *Bioceramics*, 10, pp. 53-56. doi: 10.1016/b978-008042692-1/50013-3.

Nery, E. B., LeGeros, R. Z., Lynch, K. L. and Lee, K. (1992) 'Tissue Response to Biphasic Calcium Phosphate Ceramic With Different Ratios of HA/βTCP in Periodontal Osseous Defects', *Journal of Periodontology*, 63(9), pp. 729-735. doi: 10.1902/jop.1992.63.9.729.

Okada, T., Kanai, T., Tachikawa, N., Munakata, M. and Kasugai, S. (2016) 'Long-term radiographic assessment of maxillary sinus floor augmentation using beta-tricalcium phosphate: analysis by cone-beam computed tomography', *International Journal of Implant Dentistry*. International Journal of Implant Dentistry, 2(1), pp. 0–8. doi: 10.1186/s40729-0160042-6.

Patel, N., Best, S. M., Bonfield, W., Gibson, I. R., Hing, K. A., Damien, E. and Revell, P. A. (2002) 'A comparative study on the in vivo behavior of hydroxyapatite and silicon substituted hydroxyapatite granules', *Journal of Materials Science: Materials in Medicine*, 13(12), pp. 1199–1206. doi: 10.1023/A:1021114710076.

Peters, F. and Reif, D. (2004) 'Functional materials for bone regeneration from beta-tricalcium phosphate', *Materialwissenschaft und Werkstofftechnik*, 35(4), pp. 203–207. doi: 10.1002/mawe.200400735.

Pietak, A. M., Reid, J. W., Stott, M. J. and Sayer, M. (2007) 'Silicon substitution in the calcium phosphate bioceramics', *Biomaterials*, 28(28), pp. 4023–4032. doi: 10.1016/j.biomaterials.2007.05.003.

Roberts, J. E., Bonar, L. C., Griffin, R. G. and Glimcher, M. J. (1992) 'Characterization of very young mineral phases of bone by solid state 31Phosphorus magic angle sample spinning nuclear magnetic resonance and X-ray diffraction', *Calcified Tissue International*, 50(1), pp. 42–48. doi: 10.1007/BF00297296.

Schepers, E., Clercq, M. D., Ducheyne, P. and Kempeneers, R. (1991) 'Bioactive glass particulate material as a filler for bone lesions', *Journal of Oral Rehabilitation*, 18(5), pp. 439–452. doi: 10.1111/j.1365-2842.1991.tb01689.x.

Simion, M., Fontana, F., Rasperini, G. and Maiorana, C. (2004) 'Long-term evaluation of osseointegrated implants placed in sites augmented with sinus floor elevation associated with vertical ridge augmentation: a retrospective study of 38 consecutive implants with 1- to 7-year follow-up', *The International journal of periodontics & restorative dentistry*,24(3), pp. 208— 221. Available at: http://europepmc.org/abstract/MED/15227769.

Sogal, A. and Tofe, A. J. (1999) 'Risk Assessment of Bovine Spongiform Encephalopathy Transmission Through Bone Graft Material Derived From Bovine Bone Used for Dental Applications', *Journal of Periodontology*, *70*(9), pp. 1053-1063. doi: 10.1902/jop.1999.70.9.1053.

Starch-Jensen, T. and Jensen, J. D. (2017) 'Maxillary Sinus Floor Augmentation: a Review of Selected Treatment Modalities', *Journal of Oral and Maxillofacial Research*, 8(3), pp. 1–13. doi: 10.5037/jomr.2017.8303.

Stiller, M., Rack, A., Zabler, S., Goebbels, J., Dalügge, O., Jonscher, S. and Knabe, C. (2009) 'Quantification of bone tissue regeneration employing β-tricalcium phosphate by three -dimensional non-invasive synchrotron micro-tomography-A comparative

examination with histomorphometry', *Bone*. Elsevier Inc., 44(4), pp. 619–628. doi: 10.1016/j.bone.2008.10.049.

Stiller, M., Kluk, E., Bohner, M., Lopez-Heredia, M. A., Müller-Mai, C. and Knabe, C. (2014) 'Performance of β-tricalcium phosphate granules and putty, bone grafting materials after bilateral sinus floor augmentation in humans', *Biomaterials*. Elsevier Ltd, 35(10), pp. 3154– 3163. doi: 10.1016/j.biomaterials.2013.12.068.

Suba, Z., Takács, D., Matusovits, D., Barabás, J., Fazekas, A. and Szabó, G. (2006) 'Maxillary sinus floor grafting with β-tricalcium phosphate in humans: Density and microarchitecture of the newly formed bone', *Clinical Oral Implants Research*, 17(1), pp. 102–108. doi: 10.1111/j.16000501.2005.01166.x.

Szabó, G., Huys, L., Coulthard, P., Maiorana, C., Garagiola, U., Barabas, J., Németh, Z., Hrabák, K. and Suba, Z. (2005) 'A prospective multicenter randomized clinical trial of autogenous bone versus beta-tricalcium phosphate graft alone for bilateral sinus elevation: histologic and histomorphometric evaluation', *The International journal of oral & maxillofacial implants*, 20(3), pp. 371—381. Available at: http://europepmc.org/abstract/MED/15973948.

Tadjoedin, E. S., De Lange, G. L., Lyaruu, D. M., Kuiper, L. and Burger, E. H. (2002) 'High concentrations of bioactive glass material (BioGran®) vs. autogenous bone for sinus floor elevation: Histomorphometrical observations on three split mouth clinical cases', *Clinical Oral Implants Research*, 13(4), pp. 428–436. doi: 10.1034/j.1600-0501.2002.130412.x.

Tatum, H. (1986) 'Maxillary and sinus implant reconstructions.', *Dental clinics of North America*, 30(2), pp. 207-229.

Temmerman, A., Keestra, J. A. J., Coucke, W., Teughels, W. and Quirynen, M. (2015) 'The outcome of oral implants placed in bone with limited bucco-oral dimensions: A 3-year followup study', *Journal of Clinical Periodontology*, 42(3), pp. 311–318. doi: 10.1111/jcpe.12376.

Thrivikraman, G., Athirasala, A., Twohig, C. and Boda, S. K. (2017) 'Biomaterials for Craniofacial Bone Regeneration', *Dental Clinics of North America*, 61(4), pp. 835–856. doi: 10.1016/j.cden.2017.06.003.

Timmenga, N. M., Raghoebar, G. M., Boering, G. and Van Weissenbruch, R. (1997) 'Maxillary sinus function after sinus lifts for the insertion of dental implants', *Journal of Oral Maxillofacial Surgery*, 55(9), pp. 936–939. doi: 10.1016/S0278-2391(97)90063-X.

Tinti, C., Parma-Benfenati, S. and Polizzi, G. (1996) 'Vertical ridge augmentation: what is the limit?', *The International journal of periodontics & restorative dentistry*, 16(3), pp. 220-229.

Titsinides, S., Agrogiannis, G. and Karatzas, T. (2019) 'Bone grafting materials in dentoalveolar reconstruction: A comprehensive review', *Japanese Dental Science Review*, *55* (1), pp. 26-32. doi: 10.1016/j.jdsr.2018.09.003.

Tonelli, P., Duvina, M., Barbato, L., Biondi, E., Nuti, N., Brancato, L. and Delle Rose, G. (2011) 'Bone regeneration in dentistry', *Clinical Cases in Mineral and Bone Metabolism*, 8(3), pp. 24-28.https://www.ncbi.nlm.nih.gov/pmc/articles/PMC3279056/#__sec1title.

Turco, G., Porrelli, D., Marsich, E., Vecchies, F., Lombardi, T., Stacchi, C. and Di Lenarda, R. (2018) 'Three-Dimensional Bone Substitutes for Oral and Maxillofacial Surgery: Biological and Structural Characterization', *Journal of Functional Biomaterials*, 9(4), p. 62. doi: 10.3390/jfb9040062.

Wang, H. L. and Boyapati, L. (2006) '"pASS" principles for predictable bone regeneration', *Implant Dentistry*, 15(1), pp. 8–17. doi: 10.1097/01.id.0000204762.39826.0f.

Wheeler, D. L., Jenis, L. G., Kovach, M. E., Marini, J. and Turner, A. S. (2007) 'Efficacy of silicated calcium phosphate graft in posterolateral lumbar fusion in sheep', *Spine Journal*, *7*(3), pp. 308-317. doi: 10.1016/j.spinee.2006.01.005.

Wheeler, S. L. (1997) 'Sinus augmentation for dental implants: The use of alloplastic materials', *Journal of Oral and Maxillofacial Surgery*, 55(11), pp. 1287–1293. doi: 10.1016/S02782391(97)90186-5.

Xie, C., Lu, H., Li, W., Chen, F.-M. and Zhao, Y.-M. (2012) 'The use of calcium phosphate-based biomaterials in implant dentistry', *Journal of Materials Science: Materials in Medicine*, 23(3), pp. 853–862. doi: 10.1007/s10856-011-4535-9.

Yamada, M. and Egusa, H. (2018) 'Current bone substitutes for implant dentistry', *Journal of Prosthodontic Research*. Japan Prosthodontic Society, 62(2), pp. 152–161. doi: 10.1016/j.jpor.2017.08.010.

Yao, J., Radin, S., Reilly, G., Leboy, P. S. and Ducheyne, P. (2005) 'Solution-mediated effect of bioactive glass in poly (lactic-co-glycolic acid)-bioactive glass composites on osteogenesis of marrow stromal cells', *Journal of Biomedical Materials Research - Part A*, 75(4), pp. 794–801 doi: 10.1002/jbm.a.30494.

Yaszemski, M. J., Payne, R. G., Hayes, W. C., Langer, R. and Mikos, A. G. (1996) 'Evolution of bone transplantation: Molecular, cellular and tissue strategies to engineer human bone', *Biomaterials*, 17(2), pp. 175–185. doi: 10.1016/0142-9612(96)85762-0.

Zerbo, I. R., Bronckers, A. L. J. J., De Lange, G. L., Van Beek, G. J. and Burger, E. H. (2001) 'Case report - Histology of human alveolar bone regeneration with a porous tricalcium phosphate: A report of two cases', *Clinical Oral Implants Research*, 12(4), pp. 379-384 doi: 10.1034/j.1600-0501.2001.012004379.x.

Zerbo, I. R., Zijderveld, S. A., De Boer, A., Bronckers, A. L. J. J., De Lange, G., Ten Bruggenkate, C. M. and Burger, E. H. (2004) 'Histomorphometry of human sinus floor augmentation using a porous β-tricalcium phosphate: A prospective study', *Clinical Oral Implants Research*, 15(6), pp. 724–732. doi: 10.1111/j.1600-0501.2004.01055.x.

Zerbo, I. R., Bronckers, A. L., De Lange, G. and Burger, E. H. (2005) 'Localisation of osteogenic and osteoclastic cells in porous β-tricalcium phosphate particles used for human maxillary sinus floor elevation', *Biomaterials*, 26(12), pp. 1445–1451. doi: 10.1016/j.biomaterials.2004.05.003.

Zhai, W., Lu, H., Chen, L., Lin, X., Huang, Y., Dai, K., … and Chang, J. (2012) 'Silicate bioceramics induce angiogenesis during bone regeneration', *Acta Biomaterialia*. Acta Materialia Inc., 8(1), pp. 341–349. doi: 10.1016/j.actbio.2011.09.008.

Zizzari, V. L., Zara, S., Tetè, G., Vinci, R., Gherlone, E. and Cataldi, A. (2016) 'Biologic and clinical aspects of integration of different bone substitutes in oral surgery: a literature review', *Oral Surgery, Oral Medicine, Oral Pathology and Oral Radiology*. Elsevier Inc., 122(4), pp. 392–402. doi: 10.1016/j.oooo.2016.0

I. Verzeichnis der akademischen Lehrer

- Meine akademischen Lehrer war in Philipps Universität Marburg:

Prof. Dr. med. dent. Christine Knabe-Ducheyne

- Meine akademischen Lehrer waren an der Universität von Sheffield:

Bingle, Douglas, Farthing, Franklin, Hunter, Jones, Khurram, Lambert, Speight, Stafford, Whawell.

- Meine akademischen Lehrer waren an der Universität von Tripolis:

Abuloufa, Al-Gabroun, Alhattab, Al-Hudhiri, Alkamis, Alkoom, Almshai, Alqadi, Arafa, Azoz, Elkabir, Ghirri, Hawas, Iftees, Moawia, Sassi, Sebkha, Wanis, Zindah.

II. Acknowledgment

Thank you for Aviation and Submarine Centre for supporting this project

I would like to express my thankfulness to Prof. Dr. Knabe-Ducheyne to her supervision throughout my research.

I would like to extend my gratitude to technical staff for their assistance at Experimental Orofacial medicine laboratory

I would like to thank Dr. Imran Tariq for his help with the statistical analysis

A huge thank you for all my friends in Libya, the UK and Germany especially; Soumaya, Emni, Muna, Annisa, Tamila, Nadia and Tarek.

I would like to say thank you very much for my parents and siblings; Hani, Hisham, Hitham and Halla for their support, help and encouragement.

Ultimately, I would like to express my appreciation to Oral and Maxillofacial Medicine Department at Aviation and Submarine Centre that has provided a three-year period to enable me to undertake the PhD degree at Philipps University of Marburg.